



COOLING OF SOLAR PANELS USING CHANNELS

**2023
MASTER THESIS
MECHANICAL ENGINEERING**

Mujtaba Jalal Khazaal AL-MOHAMMEDAWI

**Thesis Advisors
Assist. Prof. Dr. Erhan KAYABAŞI
Prof. Dr. Hayder Abed DHAHAD**

COOLING OF SOLAR PANELS USING CHANNELS

Mujtaba Jalal Khazaal AL-MOHAMMEDAWI

Thesis Advisors

Assist. Prof. Dr. Erhan KAYABAŞI

Prof. Dr. Hayder Abed DHAHAD

T.C.

Karabuk University

Institute of Graduate Programs

Department of Mechanical Engineering

Prepared as

Master Thesis

KARABUK

July 2023

I certify that in my opinion the thesis submitted by Mujtaba Jalal Khazaal AL-MOHAMMEDAWI titled “COOLING OF SOLAR PANELS USING CHANNELS” is fully adequate in scope and in quality as a thesis for the degree of Master of Science.

Assist. Prof. Dr. Erhan KAYABAŞI
Thesis Advisor, Department of Mechanical Engineering

Prof. Dr. Hayder Abed DHAHAD
Thesis Advisor, Department of Mechanical Engineering

This thesis is accepted by the examining committee with a unanimous vote in the Department of Mechanical Engineering as a Master of Science thesis. 23/06/2023

<u>Examining Committee Members (Institutions)</u>	<u>Signature</u>
Chairman : Prof. Dr. Hüseyin KURT (EU)
Member : Assist. Prof. Dr. Erhan KAYABAŞI (KBU)
Member : Prof. Dr. Hayder Abed DHAHAD (TU)
Member : Assoc. Prof. Dr. Engin GEDİK (KBU)
Member : Assist. Prof. Dr. Abdulrazzak A. S. AKROOT (KBU)

The degree of Master of Science by the thesis submitted is approved by the Administrative Board of the Institute of Graduate Programs, Karabuk University.

Prof. Dr. Müslüm KUZU
Director of the Institute of Graduate Programs

“I declare that all the information within this thesis has been gathered and presented in accordance with academic regulations and ethical principles and I have according to the requirements of these regulations and principles cited all those which do not originate in this work as well.”

Mujtaba Jalal Khazaal AL-MOHAMMEDAWI

ABSTRACT

M. Sc. Thesis

COOLING OF SOLAR PANELS USING CHANNELS

Mujtaba Jalal Khazaal AL-MOHAMMEDAWI

Karabük University

Institute of Graduate Programs

The Department of Mechanical Engineering

Thesis Advisors:

Assist. Prof. Dr. Erhan KAYABAŞI

Prof. Dr. Hayder Abed DHAHAD

July 2023, 71 pages

Solar energy is an essential source in this era. One of the most important applications of solar energy is solar panels; however, the problem with solar panels is that the higher their temperature, the lower their efficiency. To address this issue, it is imperative to cool the solar panels using a simple and effective cooling system. Therefore, this research conducted an experiment to explore cooling methods by implementing fluid channels on the back of the solar panel. Water and air were used as cooling fluids, and different flow rates (0.35 L/M, 0.7 L/M, and 1.4 L/M) were tested for each case. Four models with varying numbers of channels (3, 5, 7, and 9) were employed in the study, and the theoretical analysis was performed using the Ansys 22 program.

The results revealed that increasing the flow rate enhanced the cooling efficiency, with a flow rate of 1.4 L/M being the most efficient. Moreover, the cooling efficiency increased with the number of channels in the models, with the 9-channel model

demonstrating the highest efficiency. As a result, this model dissipated less heat from the solar panel, leading to improved electrical efficiency. When comparing the cooling fluids, it became evident that water cooling outperformed air cooling, exhibiting superior results.

Key Words : Solar Energy, Photovoltaic, Numerical Analysis

Science Code : 91408

ÖZET

Yüksek Lisans Tezi

COOLING OF SOLAR PANELS USING CHANNELS

Mujtaba Jalal Khazaal AL-MOHAMMEDAWI

Karabük University

Institute of Graduate Programs

The Department of Mechanical Engineering

Tez Danışmanları:

Dr. Öğr. Üyesi Erhan KAYABAŞI

Prof. Dr. Hayder Abed DHAHAD

Temmuz 2023, 71 sayfa

Güneş enerjisi, günümüzde önemli bir kaynaktır. Güneş enerjisinin en önemli uygulamalarından biri güneş panelleridir; ancak, panellerin sıcaklığı arttıkça verimleri düşer. Bu sorunu çözmek için güneş panellerini basit ve etkili bir soğutma sistemiyle soğutmak önemlidir. Bu nedenle, bu araştırma güneş panelinin arka kısmına akışkan kanalları uygulayarak bir soğutma deneyi gerçekleştirdi. Her biri için farklı akış hızları (0.35 L/D, 0.7 L/D ve 1.4 L/D) olan su ve hava, soğutma akışkanları olarak kullanıldı. Çalışmada 3, 5, 7 ve 9 adet kanala sahip dört farklı model kullanıldı ve teorik analiz Ansys 22 programı kullanılarak yapıldı.

Sonuçlar, akış hızının arttıkça soğutma verimliliğinin arttığını, en etkili akış hızının 1.4 L/D olduğunu gösterdi. Ayrıca, modellerdeki kanal sayısının artmasıyla soğutma verimliliğinin arttığı ve 9 kanallı modelin en yüksek verimliliği gösterdiği görüldü. Bu sonuç olarak güneş panelinden daha az ısı yayılmasını sağladı ve elektrik

verimliliğinin artmasına katkı sağladı. Soğutma akışkanları karşılaştırıldığında, su soğutmanın hava soğutmaya göre üstün sonuçlar sergilediği ortaya çıktı.

Anahtar Kelimeler : Güneş Enerjisi, Fotovoltik, Sayısal Analiz

Bilim Kodu : 91408

ACKNOWLEDGMENT

Foremost, I praise Allah almighty for giving me the motivation and ability to accomplish this thesis and its success.

I Want to express my sincere gratitude and thanks to my supervisors, Assist. Prof. Dr. Erhan KAYABASI and Prof. Dr. Hayder Abed DHAH for the continuous support of my MS studies through their scientific suggestions, guidance, and assistance in carrying out the present research.

My deepest gratitude goes to my parents, to whom and I am very grateful for having amazing brothers and sisters for being so close to me. I will be grateful for my brothers and sisters have always been so close to me.

In The end, I would also like to offer my special thanks to the Department of mechanical engineering at Karabuk University, and the Department of Mechanical Engineering at the University of Technology-Iraq.

CONTENTS

	<u>Page</u>
APPROVAL.....	ii
ABSTRACT.....	iv
ÖZET.....	vi
ACKNOWLEDGMENT.....	viii
CONTENTS.....	ix
LIST OF FIGURES	xi
LIST OF TABLES	xiv
SYMOOLS AND ABBREVIATIONS INDEX	xv
PART 1	1
INTRODUCTION	1
1.1. BACKGROUND.....	1
1.2. THE ADVANTAGES AND DISADVANTAGES OF USING SOLAR ENERGY.....	4
1.2.1. Advantages of Solar Energy	4
1.2.2. Disadvantages of Solar Energy.....	5
1.3. SOLAR CELL TYPES AND MANUFACTURING METHODS.....	6
1.3.1. The First Solar Cell Generation	6
1.3.2. Solar Cells Of The Second Generation.....	6
1.3.3. Third-Generation Solar Cells.....	7
1.4. OBJECTIVES	8
1.5. THESIS ARRANGEMENT.....	8
PART 2	10
LITERATURE REVIEW.....	10
2.1. INTRODUCTION.....	10
2.2. PREVIOUS STUDIES	10
PART 3	24
NUMERICAL SIMULATION	24

	<u>Page</u>
3.1. INTRODUCTION.....	24
3.2. PHYSICAL MODEL	25
3.3. GEOMETRY DESIGN	25
3.4. GOVERNING EQUATION	26
3.5. MESH GENERATION	28
3.6. SETUP.....	29
3.7. BOUNDARY CONDITIONS	31
PART 4	32
RESULTS AND DISCUSSION	32
4.1. GENERAL	32
4.2. SOLER PANEL REFERENCE.....	33
4.3. WATER COOLING SYSTEM.....	35
4.3.1. Three Channel Model	35
4.3.2. Five Channel Model	38
4.3.3. Seven Channel Model.....	40
4.3.4. Nine Channel Model.....	43
4.4. AIR COOLING SYSTEM	47
4.4.1. Three Channel Model	47
4.4.2. Five Channel Model	50
4.4.3. Seven Channel Model.....	52
4.4.4. Nine Channel Model.....	54
4.5. OUTLET TEMPERATURE AVERAGE FOR COOLING CHANNELS	57
4.6. COMPARISON BETWEEN WATER COOLING SYSTEM AND AIR COOLING SYST	58
PART 5	64
CONCLUSION AND SUGGESTION	64
5.1. CONCLUSION	64
5.2. SUGGESTION	64
REFERENCES.....	66
RESUME	71

LIST OF FIGURES

	<u>Page</u>
Figure 1.1. The efficiency of solar cells fluctuates throughout the day due to the variations in solar radiation.....	3
Figure 1.2. Temperature Influence on the Maximum Output Power	4
Figure 3.1. Ansys steps.	24
Figure 3.2. Geometry design a) For stander soler panel b) For 3 channel model c)For 5 channel model d) For 7 channel model e) For 9 channel model.	26
Figure 3.3. Details of mesh in ansys.22.	29
Figure 3.4. Form of mesh	29
Figure 3.5. Mass-flow inlet in setup.....	30
Figure 3.6. Viscous model in setup.	31
Figure 4.1. Details of Radiation Model.....	33
Figure 4.2. Temperature distribution of the solar panel reference.	34
Figure 4.3. Temperature changes with time for the reference panel.	34
Figure 4.4. Change of electrical efficiency with time for the reference panel.	35
Figure 4.5. Temperature distribution on the solar panel in 3 channel A)for 0.35L/M, B)for 0.7L/M, C)for 1.4L/M.....	35
Figure 4.6. Temperature changes with time in the solar panel at three-channel water cooling.	36
Figure 4.7. Electrical efficiency changes with time three channel water cooling...	37
Figure 4.8. Temperature distribution on the solar panel in 5 channel a) for 0.35L/M, b) for 0.7L/M, c) for 1.4L/M.	38
Figure 4.9. The temporal variation of temperature in the solar panel with a five-channel water cooling system.	38
Figure 4.10. The electrical efficiency of a five-channel water cooling system varies over time.	39
Figure 4.11. Temperature Distribution on the Solar Panel Across Different Flow Rates in Seven Channels A)for 0.35L/M, B)for 0.7L/M, C) for 1.4L/M.....	40
Figure 4.12. Temperature Variation over Time in a Three-Channel Water-Cooled Solar Panel	41
Figure 4.13. Electrical efficiency changes with time seven channel water cooling..	42

	<u>Page</u>
Figure 4.14. Temperature Distribution Across Nine Channels on the Solar Panel a) for 0.35L/M, b) for 0.7L/M, c) for 1.4L/M.....	43
Figure 4.15. Temporal Variation of Solar Panel Temperature with Nine-Channel Water Cooling.....	43
Figure 4.16. Temporal Variation of Electrical Efficiency in Nine-Channel Water Cooling System.....	44
Figure 4.17. Temperature Variation over Time in Solar Panels with Water-Cooling Channels.....	45
Figure 4.18. Time-Dependent Variation of Electrical Efficiency in Water-Cooled Solar Panels.....	46
Figure 4.19. Temperature distribution on a solar panel under three-channel air cooling conditions. a) for 0.35L/M, b) for 0.7L/M, c) for 1.4L/M.....	47
Figure 4.20. Temporal variation of temperature in a solar panel under three-channel air cooling conditions.....	48
Figure 4.21. Variation in Electrical Efficiency with three-Channel Air Cooling.	49
Figure 4.22. Temperature distribution on the solar panel utilizing a five-channel cooling system. a) for 0.35L/M, b) for 0.7L/M, c) for 1.4L/M.	50
Figure 4.23. Variations in temperature over time on the solar panel subjected to air cooling through the five-channel configuration.....	50
Figure 4.24. Variation in Electrical Efficiency with five-Channel Air Cooling.	51
Figure 4.25. Temperature distribution on the solar panel utilizing a seven-channel cooling system a) for 0.35L/M, b) for 0.7L/M, c) for 1.4L/M.	52
Figure 4.26. Variation in Temperature over time in the solar panel with seven-Channel Air Cooling.	52
Figure 4.27. Variation in Electrical Efficiency with Seven-Channel Air Cooling. ..	53
Figure 4.28. Temperature distribution on the solar panel utilizing a nine-channel cooling system a) for 0.35L/M, b) for 0.7L/M, c) for 1.4L/M.	54
Figure 4.29. Variation in Temperature over time in the solar panel with nine-Channel Air Cooling.....	54
Figure 4.30. Variation in Electrical Efficiency with nine-Channel Air Cooling.	55
Figure 4.31. Variation in Temperature over time in the solar panel in the solar panel under different air-cooling configurations.....	56
Figure 4.32. Variation in Electrical Efficiency in the solar panel under different air-cooling configurations	57
Figure 4.33. Time-dependent temperature variations in a solar panel with three-channel air and water cooling.	59
Figure 4.34. Time-dependent temperature variations in a solar panel with five-channel air and water cooling.	60

	<u>Page</u>
Figure 4.35. Time-dependent temperature variations in a solar panel with seven-channel air and water cooling.	60
Figure 4.36. Time-dependent temperature variations in a solar panel with nine-channel air and water cooling.	61
Figure 4.37. Electrical efficiency changes over time in a solar panel equipped with three-channel air and water cooling.	61
Figure 4.38. Electrical efficiency changes over time in a solar panel equipped with five-channel air and water cooling.	62
Figure 4.39. Electrical efficiency changes over time in a solar panel equipped with seven-channel air and water cooling.	62
Figure 4.40. Electrical efficiency changes over time in a solar panel equipped with nine-channel air and water cooling.	63

LIST OF TABLES

	<u>Page</u>
Table 3.1. The PV panel specifications.....	26
Table 3.2. Inlet boundary conditions.	31
Table 4.1. Average Temperature for cooling channels	57
Table 4.2. Compration between this study and another study	63

SYMOOLS AND ABBREVIATIONS INDEX

SYMOOLS

P	: power	w
I	: current	A
V	: voltage	v
η	: efficiency	
η_{el}	: Electrical efficiency	
G	: radiation intensity	w / m ²
A	: Area	m ²
u,v,w	: velocity components	
p	: pressure	N/m ²
g	: Acceleration of gravity	m/s ²
ρ	: density	Kg/m ³
μ	: Dynamic viscosity	Ns/m ²
V	: velocity	m/s
Re	: Reynolds Number	
μ_t	: Eddy viscosity	Ns/m ²
$\bar{\tau}$: stress tensor	N/m ²
u_i	: component of velocity	m/s
Cp	: Specific Heat	kJ/kg · °C
K	: Thermal conductivity	W/m · °C
x, y, z	: Space coordinates in cartesian system	
α	: Thermal diffusivity	m ² /s
q	: Heat-transfer rate	kJ per unit time
t, T	: Temperature	°C

ABBREVIATIONS

Al	: Aluminum
CeO ₂	: cerium oxide
CO ₂	: carbon dioxide
Eff:	: efficiency of solar cell
PV	: Photovoltaics
PVT	: Photovoltaics Thermal
BC	: Black-Chrome
Ni-Co	: Nickel-cobalt
HI	: heat index
CFD	: Computational fluid dynamic
CPV	: Concentrating photovoltaics
GNP	: graphene particles

PART 1

INTRODUCTION

1.1. BACKGROUND

Renewable fuels are increasingly being utilized to meet global production and power demands, with renewable energy becoming more in-demand due to its eco-friendliness compared to non-renewable energy sources, which have had noticeable adverse effects on our environment, especially in nations where such resources are prevalent. This increasing demand for renewable energy has become even more crucial in light of the harmful impact of greenhouse gases on the environment caused by continued reliance on fossil fuels to meet the world's energy needs.

Among cleaner technologies used in the workplace, rooftop solar (PV) electricity stands out as one of the most frequently adopted and likely the most prevalent [1–6]. A solar PV panel consists of an array of solar cells that efficiently convert sunlight into electrical energy. The ongoing advancements in solar technology have made it more accessible and affordable, resulting in its widespread adoption. However, despite its global popularity, solar PV has some limitations, such as reduced efficiency at higher operating temperatures, low energy conversion rates, and the accumulation of dust on the module's surface, all of which negatively impact its overall performance [7–9]. Elevated temperature of a PV panel affects its operational characteristics, leading to reduced energy output. It is estimated that PV efficiency decreases by 1% for every 5°C increase in ambient temperature [10].

Another significant reason for cooling PV panels is to enhance their endurance and reduce degradation rates. By implementing appropriate cooling techniques, the

lifespan of a PV panel can be significantly extended, with some studies suggesting an increase from the average 25-30 years to over 48 years [11].

Efficient cooling of solar panels is vital to ensure their optimal performance. Excessive heat can directly and indirectly degrade solar cells, potentially reducing the quality of PV power output. Thus, keeping the surface temperature of the solar cells as low as possible is essential. Jet conditioning devices are employed during operation to maintain the efficiency of PV panels by controlling temperature levels. The coolant temperature has a substantial impact on the performance and efficiency of solar PV systems, making it crucial to investigate various methods of regulating solar panel temperatures.

Numerous experimental and numerical studies have been conducted to minimize heat transfer [12]. Researchers have explored various techniques to enhance the overall performance of PV panels. For instance, Grubiic et al. (2016) reviewed advancements in solar cell (PV) panel cooling systems and temperature management. In a similar study, authors analyzed an additional cooling strategy using water spray on the edges of photovoltaic (PV) panels [13]. The experimental findings revealed that under peak solar energy conditions, the application of water spray resulted in a 7.7% increase in electrical grid output and a 5.9% drop in PV panel exergy efficiency. When the front and rear of the PV panel were cooled simultaneously with high spray rates, the average panel temperature decreased from 54°C to 24°C. The corresponding power losses were calculated to be 2.7, 3.5, and 4.2 W for spray rates of 144, 189, and 225 L/h, respectively. An economic feasibility analysis for the suggested water spray cooling technology was also performed [14].

In another study, water was sprayed onto solar cells to explore the potential of enhancing the performance of photovoltaic water pumping systems, leading to an increase in the solar module's efficiency from 3.26% to 12.5% [15]. Moharram et al. investigated a PV panel cooling system using water gushing [15]. When the PV panel's temperature reached the permissible limit, a computer model was utilized to initiate cooling (MAT). A cooling model was developed to assess the time required to cool PV panels to the recommended average operating temperature of 35 degrees Celsius.

Two models were used for this purpose: the heating rate model and the cooling rate model, both of which were empirically validated [16].

In regions like the Middle East, particularly the Arabian Gulf, where high temperatures during summer can exceed the specified limits for solar panels, the efficiency of these panels may decline, leading to reduced electricity output [17].

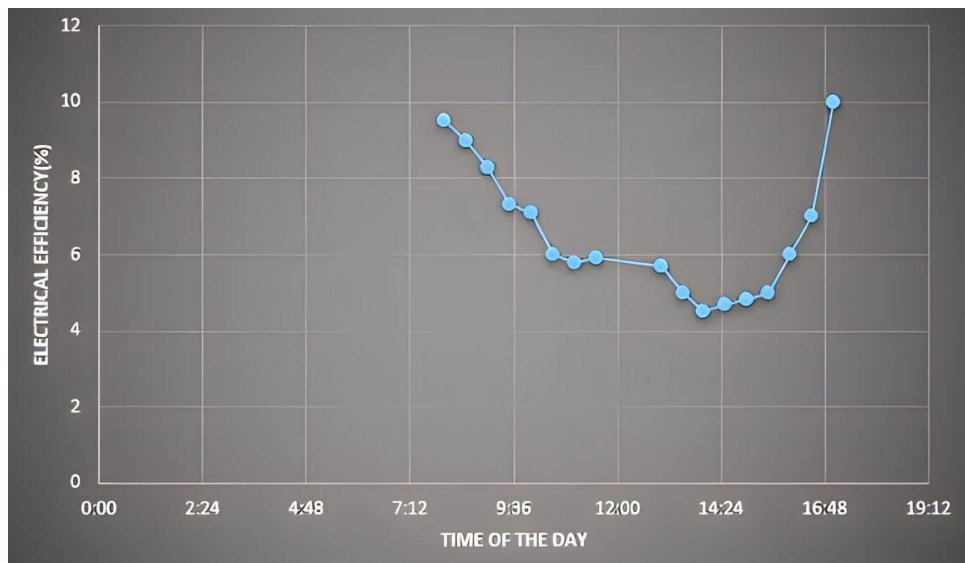


Figure 1.1. The efficiency of solar cells fluctuates throughout the day due to the variations in solar radiation.

To enhance solar power generation, the cost of increasing the number of solar panels is typically a more significant operational expense than the overall land utilization. High-concentration solar thermal and photovoltaic (PV) systems require cooling to maintain their output power. The amount of solar energy harnessed and analyzed plays a crucial role in this process, making solar cooling systems an essential consideration to ensure efficient power generation. By implementing a microcontroller-based water spraying cooling system, the equipment costs can be reduced, encouraging the wider adoption of solar cooling technologies. Additionally, local solar time affects the performance of solar panels, with a progressive increase in partial shading from 06:00 to 12:00 and a subsequent decrease from noon until around 19:00. These variations in shading can lead to reduced power production due to high heating rates [18] [19].

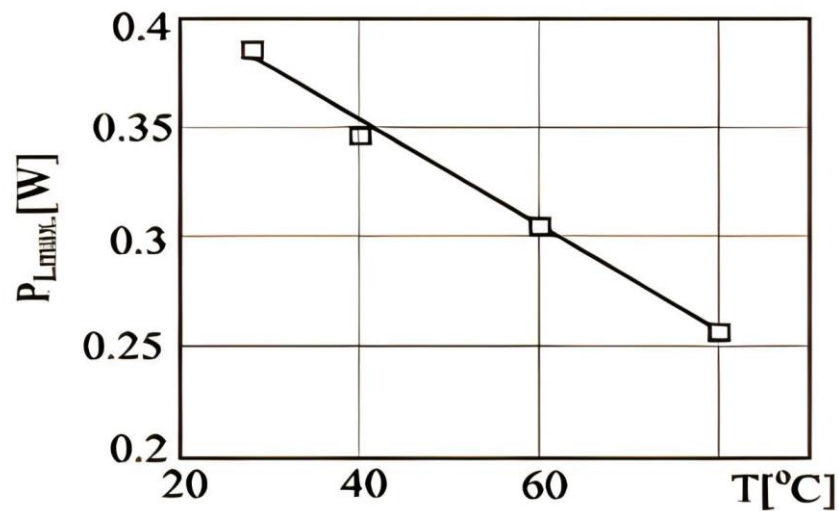


Figure 1.2. Temperature Influence on the Maximum Output Power.

1.2.THE ADVANTAGES AND DISADVANTAGES OF USING SOLAR ENERGY

Solar energy, like other energy sources, has its own set of advantages and disadvantages.

1.2.1. Advantages of Solar Energy

Solar energy is abundant and virtually limitless: The sun serves as an infinite energy source, and the amount of solar radiation reaching the Earth exceeds humanity's energy demands by several times.

Cost-effective and free to use: Solar energy is available for free, and its usage is primarily limited by the initial investment in solar panels and equipment.

No need for extensive transmission and distribution: Solar energy is dispersed globally and reaches everyone without the need for complex transmission and distribution systems.

Relatively uniform distribution based on latitudes: Despite variations between the equator and poles, solar energy distribution is generally consistent according to geographical regions, facilitating its study, utilization, and information exchange.

Versatile energy conversion: Solar energy can be converted into various forms, including thermal, mechanical, and electrical energy, providing flexibility in its applications.

Unique applications in human and plant life: Solar energy finds specialized applications in specific areas like mega projects reliant on water evaporation, photosynthesis, and others.

Environmentally friendly: Solar energy is a clean and non-hazardous source of energy, making it environmentally sustainable [20].

1.2.2. Disadvantages of Solar Energy

Lower intensity per unit area: Solar energy has a relatively low intensity per unit rooftop compared to other energy sources.

Inconsistency during the day: Solar energy is only available for a limited number of hours each day, which can pose challenges for its consistent utilization.

Lack of consumer awareness and understanding: The relevance of solar energy might not be well understood by consumers, necessitating educational initiatives to promote its adoption.

Potential lifestyle adjustments: The transition to a solar energy system may require significant changes in some societal and lifestyle aspects established by traditional energy systems developed during industrialization.

1.3. SOLAR CELL TYPES AND MANUFACTURING METHODS

1.3.1. The First Solar Cell Generation

Solar cells are predominantly made of semiconductor materials, with crystalline silicon being the most common, accounting for approximately 90% of solar cell production. There are two types of silicon cells used in solar panels:

Monocrystalline silicon cells: These cells consist of a single silicon crystal and have an efficiency of converting incoming sunlight into electrical energy at around 17-18%.

Polycrystalline silicon cells: Made of various crystals formed by melting silicon and cooling it in graphite molds. These cells represented approximately 48% of global production in 2008, with an efficiency of 12-14%.

The process of manufacturing silicon cells typically starts with the production of polysilicon, the primary material used in semiconductors. Polysilicon is cast or hammered into blocks, then cut into thin slices using wire saws, with standardized dimensions. The plates are cleaned and treated with phosphorous to form a layer of negative semiconductors that reduces sunlight reflection. Additional layers of chemicals are applied to reduce reflection and increase sunlight absorption, followed by the use of aluminum testing chips before assembly into solar panels with glass coatings to protect the semiconductors and enhance their absorbency and reduce reflection.

1.3.2. Solar Cells of The Second Generation

Second-generation solar cells include morphological cells and thin-film cells, which are more cost-effective than crystalline silicon cells but less efficient. The types of second-generation solar cells are as follows:

Amorphous silicon cells: Used in devices like calculators, these cells are made at lower temperatures and have thin silicon layers (up to one micrometer) deposited on plastic

surfaces. The efficiency of amorphous silicon cells ranges between 4-8%, and they can operate effectively at high temperatures and under varying weather conditions.

Cadmium telluride cells: These cells use a thin coating of cadmium telluride to convert sunlight into electrical energy. The efficiency of these cells ranges between 9-11%. However, environmental concerns due to cadmium toxicity may limit their usage in the solar cell industry.

Copper-indium-gallium-diselenide cells: These cells have an efficiency of 10-12% and are manufactured by depositing thin layers of copper, indium, gallium, and diselenide on glass or plastic, with electrodes placed in front and behind the cell to collect electric current. Their high absorption coefficient allows them to effectively absorb sunlight.

1.3.3. Third-Generation Solar Cells

The third generation of solar cells includes innovative species that are currently in research and development, and have not yet reached commercial industrialization. Examples of third-generation solar cells include:

Nano-solar cells: These cells work by producing semiconductor material crystals with microscopic dimensions measured in nanometers, and their efficiency ranges between 7-8%.

Polymer-based solar cells: Manufactured from polymeric substances that absorb solar radiation, these cells have an efficiency range of 3-10% and are more cost-effective than silicon solar cells.

Dye-sensitized solar cells: Comprising a thin layer of titanium dioxide for the negative semiconductor and a thin layer of nickel oxide for the positive semiconductor, these cells are easy to install.

Concentrated solar cells: These cells use multiple mirrors and lenses to generate high thermal energy for heat engines, achieving an efficiency of up to 40% and being thermally stable.

1.4. OBJECTIVES

The main objectives of this study are as follows:

- To investigate the cooling effect on solar panels by comparing panels with cooling and panels without cooling using four different models.
- To utilize the Ansys 22 program to simulate, model, and calculate the changes in the solar panel when coolant flows through the channels.
- To provide an illustration of the solar panel's shape used in the study, created using the SolidWorks program.

1.5. THESIS ARRANGEMENT

The thesis will be organized into the following sections:

Part One: Introduction

This section will provide general illustrative information about solar cells, including drawings and a simplified explanation of the research study.

Part Two: Literature Review

This part will review previous studies related to the topic, presenting their results and illustrations that are relevant to the current research study.

Part Three: Numerical Analysis and Results

In this section, the research findings will be presented, obtained through numerical analysis using the Ansys program.

Part Four: Discussion and Comparison

The results will be discussed and compared to draw meaningful conclusions about the cooling effect on solar panels.

Part Five: Conclusions and Summary

This section will provide the concluding remarks based on the discussion of results and will summarize the research study. Additionally, a list of references used in the thesis will be included.

PART 2

LITERATURE REVIEW

2.1. INTRODUCTION

Numerous efforts have been made to enhance the performance of solar panels through cooling methods. Various approaches have been explored, including altering the design shapes, using different cooling fluids, and utilizing diverse materials. The primary objective of these endeavors is to increase the efficiency of solar panels and ensure their optimal functioning. Temperature has a significant impact on the effectiveness of solar panels, with efficiency gradually decreasing as temperatures rise. To investigate and analyze the thermal performance of solar panels, as well as to compare different types and designs, numerical research and Computational Fluid Dynamics (CFD) simulations have been extensively employed. CFD simulations provide in-depth analysis and higher accuracy in studying the solar panel system. Based on the simulation results, appropriate measures have been identified and implemented to enhance the efficiency of solar panels.

2.2. PREVIOUS STUDIES

In the academic literature, substantial research has been dedicated to the cooling of photovoltaic (PV) panels, which is of utmost importance due to its significant impact on panel efficiency. Several studies have been conducted to explore various cooling methods to maintain panel efficiencies within specified values. In one study by Feyzullah Behlül, Erhan KAYABASI, et al. (2018) [1], a comprehensive literature review was presented, providing insights into the current state of technological advancements in cooling choices. The study also analyzed the strengths and weaknesses of previous research and identified promising techniques for future PV panel applications. Additionally, the researchers investigated the future prospects of

PV panel cooling, emphasizing the importance of achieving lower working temperatures to enhance operational efficiency [23].

Dacheng Li et al. (2021) [2] focused on the impact of dust deposition and heat on PV performance. They proposed a condensed gas device to improve solar PV panel efficiency and examined models for dust adhesion, detachment, and air temperature changes. The study explored the potential of using compressed air discharge for PV power output control and presented a test verification system. The findings highlighted the significance of implementing cleaning and cooling mechanisms, such as airflow duration, surface particle cleaning, and power generation efficiency, to enhance the net power output of PV panels and contribute to energy decarbonization [24].

Ephraim Bonah et al. (2021) [3] addressed the issue of PV module efficiency deterioration caused by heating. They proposed a dual surface cooling method for PV modules using a porous pipe and capillary action to collect and move water along the back surface of the device. The experimental results demonstrated a substantial temperature reduction, improved electricity production, and a notable increase in the cooled PV module's efficiency compared to an uncooled module. The recommended cooling strategy showed great potential for enhancing the energy yield of PV systems [11].

In another study, Fahad Al-Amri et al. (2022) [4] conducted an experimental analysis of temperature controllers and cooling systems for PV panels under demanding conditions. They evaluated the efficiency of heat sink and thermal storage heat sink approaches for cooling PV cells. The study concluded that the heat sink-based PV panel configuration was more effective in withstanding severe environmental climate conditions, leading to enhanced heat transfer and uniform dissipation, thereby increasing PV panel efficiencies [25].

Faruk Yesildal et al. (2021) [5] focused on optimizing the parameters for applying air-assisted water spray on PV module surfaces to prevent a decline in electrical efficiency caused by cell material heating. The study utilized the Response Surface Method to identify the optimal settings for maximum electrical efficiency, considering

parameters such as spraying time, spray flow rate, nozzle air flow rate, nozzle pressure, panel distance, and solar irradiance. The findings provided valuable associations between these parameters and electrical efficiency, contributing to advancements in PV panel performance [16].

A. Almuwailhi et al. (2021) [6] investigated the effects of natural convection, induced thermal conduction, and evaporative cooling on the performance of PV panels. Through experimentation with different cooling methods, they observed that cooling significantly increased the output and efficiency of the PV panels. Notably, forced convection cooling with air at a specific speed led to the highest increase in daily energy production and efficiency [26].

Aly M. A. Soliman et al. (2019) [7] designed an experimental setup to assess the impact of a heat sink cooling system on solar cell performance. The investigation involved using halogen lights to simulate solar radiation at various doses and employing natural and forced air cooling methods on the heat sink. The results showed that employing a heat sink cooling system improved the efficiency and power of the solar cell system, particularly when utilizing forced air cooling [27].

C. Ramesh et al. (2022) [8] conducted a study focusing on the effectiveness of a sunlight absorber panel with a reflector in solar thermal systems. The research explored different absorbers to enhance thermal efficiency, and it also investigated the use of coated panels as coverings for solar absorbance panels. Black-chrome and nickel-cobalt coatings were applied to copper photoanodes, and reflectors were utilized to increase solar radiation incident on the absorber. The thermal efficiency of solar panels was considered as the response in the experiment, while flow rate, collector angle, and reflector angle were treated as process variables. The Behnken design methodology was used for data collection from real-world experiments, and Analysis of Variance (ANOVA) was performed on the collected data. The study revealed that the Ni-Co coated panel improved the thermal efficiency of the absorber panel and reflectors by 89.3 percent [28].

Hamdi Ayed et al. (2021) [9] investigated the thermal and power output of novel-shaped solar panels, including Pyramid, Hexagonal, and Conical geometries with equal dorsal borders. Forced air flow was employed to cool these differently shaped structures, and a computational fluid dynamics (CFD) software was used for simulation. The study compared the thermal performance of the different shapes and found that the conical rounded solar panels outperformed the others, showing the lowest temperature, about 10.5 degrees Celsius lower than the pyramid-shaped panel [29].

Mamadou Simina Drame et al. (2021) [10] collected dust samples from identical photovoltaic arrays near Dakar and analyzed their structural properties. The research aimed to assess the impact of dust on the efficiency of photovoltaic panels. The dust samples were found to be a complex mixture of various elements, with silica and calcite being the main components. The study revealed that this dust, which reflects more than 70% of the irradiance, has a semi-structure with varying diameters and compositions, making it a significant contaminant affecting solar energy systems [30]. In a study conducted by Sodhi et al. (2022) [11], it is emphasized that the success of mitigating global warming and achieving sustainable development largely hinges on the reduction of CO₂ emissions through the expansion of Photovoltaic (PV) power generation. While there has been a recent increase in PV installations in both residential and larger-scale settings, it is expected that the rate of solar panel installations will accelerate significantly in the near future, driven by various factors. These factors include:

- Declining panel costs due to technological advancements and improved manufacturing efficiencies on a larger scale.
- Government initiatives and incentives promoting the adoption of solar innovations in their early stages.
- The continuous improvement in power density of solar panels, making them more efficient in converting sunlight into electricity.
- An increase in electric bills in certain cases due to the phasing out of cheaper, high-emission energy sources.

Despite the promising growth of solar panel usage, one crucial aspect that has received inadequate attention is the end-of-life management of solar panels. Most commercially available panels have a lifespan of over twenty years, leading to a perceived lack of urgency in finding appropriate solutions. However, the research demonstrates the significance of addressing this issue based on economic considerations and other factors.

In light of these challenges, the study proposes a new framework for analyzing existing solar panel products in terms of their functional and physical architecture. The objective is to group these items into new assembly-oriented product families, which would optimize existing assembly lines and facilitate the creation of new ones [31]. This approach aims to enhance the overall efficiency and sustainability of solar panel production systems, considering both economic and environmental implications.

Man-Wen Tian et al. (2021) [12] conducted a study to model and compare the economic and exergy performance of two types of solar panels: PV (Photovoltaic) and PVT (Photovoltaic-Thermal) with a cooling system. The cooling system utilized MgO/water as the working fluid, and copper tubes were arranged at the bottom of the PVT coolant to cool the panel while producing hot water. The researchers employed Simulink software and the finite element method for numerical analysis and simulation of the solar panels. Financial evaluation was carried out using an in-house MATLAB code, and meteorological data from China were used for the analysis. The study considered various settings, including different volume percentages of nanoparticles (ranging from 0 to 1) and fluid velocities (ranging from 0.5 to 4 lit/min).

The findings revealed that increasing the flow of nanofluid in the cooling system effectively cooled the solar panel while impacting the amount of exergy produced. The inclusion of nanoparticles significantly increased the exergy output, particularly at low nanofluid flow rates. The changes in exergy efficiency with variations in the volume fraction of nanoparticles and flow rate showed a similar trend to that of exergy output. Specifically, the study demonstrated that increasing the flow rate from 0.5 to 4 lit/min resulted in a 2.03 percent reduction in efficiency. However, at a volume flow rate of 0.5 lit/min, the addition of 1% nanoparticles improved exergy efficiency by 0.45%.

The economic analysis revealed that the capital recovery time was six years for PV and four years for PVT solar panels [32].

In another study by Muji Setiyo et al. (2021) [13], the focus was on the potential hazards associated with high temperatures in cars parked in the sun. The researchers investigated the properties of a solar cell-based cabin cooling system for automobiles parked under sunlight. Four ST32M100W-FLP photovoltaic systems were utilized to activate the evaporator blower when mounted on the car roof. The blower operated in two modes, with different blowing speed levels 1 ($m = 0.0086 \text{ kg/s}$) and level 2 ($m = 0.0114 \text{ kg/s}$), and with or without the addition of external air. The study showed that the car cabin cooler could effectively lower the interior temperature by 9.8 degrees Celsius. The article discussed the latent and perceptible cooling effects, heat index, and temperature drop. It was observed that the car's ability to cool off when parked in the sun from noon until three in the afternoon was influenced by the amount of sensible heat released as humidity increased. Ultimately, the car's interior chiller had the potential to reduce the thermal index (HI) from hazardous and highly harmful to dangerous and extremely cautious levels [33].

Opeyeolu Timothy Laseinde et al. (2021) [14] highlight the growing use of microgrids as electricity networks due to the increasing demand for electricity from main grids. Solar farms have gained prominence as a clean, sustainable, and renewable energy source, and their global economy has expanded significantly during the fourth industrial revolution, as more countries explore this technology. However, solar panels are exposed to high temperatures from the sun, which negatively impacts their thermal regulation and slows down PV systems. Excessive heat absorption limits the energy production capacity of solar cells, especially in concentrating Photovoltaic (PV) installations. The study focuses on an innovative solution for automatic spraying, which optimizes the cooling of solar panels and addresses the challenges encountered during hot weather conditions. An Arduino board is used to power a microcontroller-based thermal control water spraying system, effectively increasing the extraction efficiency. The study presents a thermal control algorithm designed to enhance the efficiency of the solar panel array by 16.65 percent [18].

In a study conducted by Rajvikram Madurai Elavarasan et al. (2022) [15], the researchers explore the issue of solar heat dissipation in Photovoltaic (PV) panels. While PV panels convert some solar radiation into electricity, the majority of the energy is converted into heat (>70%), leading to increased panel temperature and reduced maximum power and coefficient of performance. Efficient thermal control is crucial for maximizing the performance of solar photovoltaics. The article reviews recent studies and various design approaches, concepts, operational methodologies, and techniques aimed at addressing this challenge. The research covers proactive and reactive temperature treatment systems and provides an analysis of improving photovoltaic panel function. Additionally, the characteristics, advantages, disadvantages, and application areas of heat transfer methods utilizing air, water, heat pumps, phase change substances, and nanofluids as heat-exchange mediums are examined. The study also discusses hybrid photovoltaic heating (Concentrated solar) collectors, which recover heat generated from solar systems using a coolant, showing potential for enhancing the conversion of solar energy. The comprehensive insights provided in the article can be valuable for researchers, developers, vendors, industrialists, and specialists in planning, manufacturing, applying, and achieving better PV systems [34].

n a study conducted by Rouhollah Salehi et al. (2021) [16], the importance of renewable energy sources, particularly solar energy, is acknowledged. However, one of the challenges in generating electricity from solar energy is the increase in surface temperature of solar cells caused by ambient conditions, leading to a reduction in the efficiency and quality of solar PV systems. Each degree rise in ambient temperature results in a 0.5 percent decrease in the efficiency of PV panels. To address this issue, the study examined solar panels and cooling systems, comparing two proposed cooling methods: natural cooling and the use of a thermoelectric module. The researchers utilized forced convection to assess the stability of these cooling methods. The findings indicated that by combining a thermoelectric module with a heater, solar panels' power and efficiency could be increased by 10.50 percent each. During the test period, the average temperature of the solar panel was 10.04 degrees Celsius lower than under normal working conditions, demonstrating the potential of designing industrial solar

panels with effective cooling systems to enhance overall efficiency by reducing excess solar radiation and improving panel performance [35].

In another study by Swar A. Zubeer et al. (2022) [17], the efficiency of different solar panel systems was examined experimentally and numerically. The tests were conducted in Duhok, northern Iraq, on a sunny day with an average ambient temperature of 32.6 degrees Celsius and sun radiation of 930 W/m². The researchers used MATLAB/Simulink modeling to analyze the PV module equations and production data sheet. The study compared standard solar panels, concentrating PV (CPV) systems, and water-cooled CPV systems. The results showed that the final panel temperature of the water-cooled CPV system was significantly lower (36.5 degrees Celsius) compared to the CPV system (64.1 degrees Celsius) and standard solar panels (57.5 degrees Celsius). Moreover, the power output of the water-cooled CPV and CPV systems increased by 24.4 percent (effectively 23 percent) and 10.65 percent, respectively. The electronics efficiency of the solar panel was also improved from 14.2 percent to 17 percent using the parabolic trough and chilled water. The open-circuit voltage and line current of the ocean CPV system were expanded by 9 percent and 5.2 percent, respectively. The study demonstrated good agreement between the measured and predicted results, showcasing the potential of water-cooled CPV systems for enhancing solar panel efficiency and performance [36].

In a study conducted by TSY Moh et al. (2020) [18], the focus was on addressing the issue of ineffective heat on the surface of PV solar panels during the solar-to-electricity energy conversion process. This phenomenon leads to the generation of "by," which negatively impacts the output efficiency of the PV solar panel. The researchers found that PV temperature and output efficiency have an inversely correlated relationship, meaning that higher temperatures result in lower overall output efficiency of electrical parameters. Therefore, it is crucial to maintain a shallow temperature for PV panels to maximize their output efficiency.

To achieve efficient cooling, the study employed novel nanomaterials, specifically graphene particles (GNP), in a liquid solution known as graphene nanofluids. The research involved using multiple micro-sized channels in direct contact with the

exposed backside of the PV solar panel. GNP nanofluids were continuously flowed inside these channels to cool the flat solar panel. Previous simulation studies suggested that utilizing multiple channels with the same volume can maximize the cooling effects of graphene nanofluids.

The study demonstrated that GNP nanofluids exhibit promising cooling efficiency for PV solar panels due to their improved thermo-physical properties compared to water-based cooling solutions. As a result, the cooling efficiency of GNP is expected to increase further in the future. Additionally, the research explored the effects of varying pumping flow rates on the cooling performance of the system [37].

In a study by Talib K. Murtadha et al. (2022) [19], the researchers aimed to enhance the efficiency and functionality of a photovoltaic/thermal system by cooling the solar panel. High temperatures on the upper surface of photovoltaic panels lead to a loss of efficiency and overall output power. To address this, the study utilized TiO₂ nanoparticles nanofluid in a two-pass cooling system. Five photovoltaic panels were tested with different concentrations of TiO₂ nanofluid (1 weight percent, 2 weight percent, and 3 weight percent), as well as with water cooling and without any cooling (uncooled state).

The results showed that the most efficient cooling technique was achieved using the highest concentration of nanofluid (3 weight percent), which resulted in a cooling efficiency of 19.23 percent. The temperature difference between the output and inlet of the cooling fluids varied depending on the nanofluid concentration, with the 3 weight percent concentration producing the desired results (7.3, 7.8, 8.3, and 8.6 degrees Celsius). Compared to the uncooled photovoltaic panels, the cooling system significantly lowered the surface temperatures of the solar panels by 19.0 percent. The data were collected using a fluid rotating twice at a 30-degree tilt angle, and it was observed that higher nanofluid concentrations led to better heat extraction [38].

In another research by Xinpeng Zhao et al. (2022) [20], the focus was on developing glazing panels, such as windows, curtain walls, and skylights, that can dynamically control the amount of sunlight entering a building to reduce energy consumption. The

researchers presented a reconfigurable dual-mode reflectance glazing panel achieved by reversible electro-polymerization of a silver layer on transparent glass. This glazing panel demonstrated a higher total thermal efficiency of 89 percent compared to conventional glazing panels with only 7 percent total thermal efficiency. On a springtime day with 560–970 W/m² total solar irradiation, the silver film-coated glass achieved a total thermal efficiency of 20–60 W/m². Moreover, on a winter day with 540 W/m² of solar irradiation, the transparent glazing absorbed only 13% of sunlight while allowing 70% to pass through, resulting in a net surface warming of 400 W/m². The simulations suggested that implementing such dynamic glazing panels in a standard-size office block (5,000 m²) could reduce annual energy consumption for heating and cooling by up to 23 percent in 15 US cities [39].

In a study conducted by Zeyad A. Haidar et al. (2018) [21], the researchers investigated the effect of evaporative cooling on solar photovoltaic (PV) panels. They devised a simple and effective experimental setup to test the absorption of heat generated by a PV module and its subsequent removal through evaporative cooling. The back surface of the PV panel was kept moist and exposed to the environment, and water was gravity-fed to the back of the panel from a tank. The experiments were conducted under real-world conditions in Riyadh. The results demonstrated that the evaporative cooling strategy led to a thermal reduction of more than 20 degrees Celsius and an increase in electrical power generation efficiency of approximately 14 percent, compared to a reference PV panel. The findings were analyzed to ensure their accuracy and reliability [40].

In an article by Vivek Mohan et al. (2022) [22], India's consumer-centric solar PV business strategy was analyzed. The study focused on policy measures aimed at promoting stakeholder benefits and encouraging household solar power installations. The authors examined the recommended Feed-in Tariff (FiT) rates, PV capacity, and Average Benefit Rate (ABR) within the policy framework to maximize advantages for consumers/prosumers and the utility. The research used case studies of three home prosumers to analyze demand and generation profiles and develop profit-and-savings models for utilities. Multi-objective decision variables, such as FiT, generation capacity (as a function of demand), and ABR, were evaluated to find Pareto-optimal

consumer and utility benefits and determine fair tradeoffs. The study considered the impact of tariff and FiT rates on consumer savings and the environment, as well as utility income. Decision-making tools were created for policymakers based on the results [41].

In a study by Yinxiao Li et al. (2022) [23], the researchers explored the challenges of integrating distributed photovoltaic (PV) systems into power distribution networks. They proposed the use of dynamic thermal rating (DTR) to evaluate the transfer capacity of power distribution equipment based on current weather conditions, which can increase installed PV capacity and net revenues. Through case studies in different regions, including Texas, Switzerland, and China, the researchers demonstrated that DTR on switchgear equipment can lead to a significant increase in installed PV capacity (15%–27%) and net revenues (4%–27%). Moreover, the study revealed that under PV policies with import duties for extra electricity fed into the grid, the use of DTR becomes more profitable and is positively impacted by climate change. DTR is suggested as a more cost-effective alternative to energy storage systems for enhancing the integration of distributed PV systems into distribution networks [42].

In a study by Mohamed R. Gomaa et al. (2021) [24], the researchers addressed thermal, economic, and reliability concerns associated with high-performance Photovoltaic/Thermal (PV/T) systems. They found that PV/T systems perform better in high-irradiance areas compared to standard PV systems. To improve the performance of PV/T systems, an optimal cooling system was modeled to remove excess heat from the PV module. The study considered two types of cooling cross-finned channel boxes: thin (3 mm) and thick (15 mm). Various irradiation levels and cooling water flow rates were analyzed to understand their effects on the PV cell and output cooling water temperatures. Numerical simulations were conducted using ANSYS, a finite-elements-based software, in a 3-D model. The findings showed that at a cooling fluid flow rate of 3 L/min, both thin and thick box heat exchangers led to lower average surface temperature distribution of PV/T systems and outlet cooling water temperature. Under a solar irradiation of 1000 W/m² and ideal flow rate, the

average surface and water-cooling temperatures for thin box heat exchangers were 30.7 degrees Celsius and 38.9 degrees Celsius, respectively [43].

In another study by Furqan Tahi et al. (2021) [25], the focus was on achieving sustainability through an increase in the market share of renewable energy sources, particularly photovoltaics (PV). PV is considered more economically viable due to its lower cost, ease of installation, and higher reliability compared to other renewable energy sources. However, PV is also more dependent on weather patterns. The study explored the performance of different types of PV panels, particularly monofacial PV and bifacial PV. Bifacial PV, which offers a higher energy yield at a lower price, is expected to overtake monofacial PV as the market leader. The researchers used detailed mathematical models to estimate the PV output and analyzed the performance of both monofacial and bifacial PV panels under different climatic conditions. The climate model predicted weather patterns for the years 2050 and 2080, and the study provided and examined average hourly solar irradiance and energy yield responses [44].

In a study by Kara Kessling et al. (2017) [26], the feasibility of combining solar panels with green roofs was investigated on the rooftop of the ARC at the University of Illinois at Urbana-Champaign. The goal was to determine if this combination is more cost-effective and environmentally friendly compared to installing either solar panels or green roofs alone. The study considered three sustainable rooftop solutions: solar panels and a green roof, only solar panels, or only a green roof. The calculations assumed that the roof would first be covered with greenery, and then solar panels would be placed three feet above the vegetation, covering 90% of the roof with both features.

The financial analysis showed that the payback period for solar panels alone was 13 years, for a green roof alone was 73 years, and for combining the two was also 13 years. Despite the higher initial cost, the combination of solar panels and green roofs proved feasible due to its relatively short payback period compared to installing only solar panels. Combining the two sustainable features provided additional benefits, such as increased plant diversity on the green roof, reduced solar panel maintenance,

and a better climate for solar panels to perform efficiently. Overall, this initiative helped the university in reaching its iCAP goals [45].

In a study by Yongwang Zhang et al. (2021) [27], the focus was on lowering building energy consumption and achieving ecological sustainability through the use of solar energy and green building practices. With the increasing concerns of global warming, environmental degradation, and resource scarcity, solar energy has emerged as a clean and renewable energy source. The study investigated how buildings can adapt to the climate and improve building quality by incorporating green building concepts and utilizing solar energy in a primary school prize design. The aim was to create low-energy, green, ecological, and sustainable structures through renovation [46].

In another research by Byoungsu Ko et al. (2018) [28], the study explored the concept of radiative cooling techniques as a means to reduce energy consumption in response to global warming. Radiative cooling involves releasing heat to the outer space, but it has been inefficient during the daytime due to bright sunlight. However, the development of metamaterials has made radiative cooling under direct sunlight achievable. The key principles of metamaterial-based radiative cooling are near-perfect reflection in the visible and near-infrared spectrums and high heat emission in the infrared atmospheric window region. The research reviewed various materials and designs used for radiative cooling and discussed their potential as replacements in the existing cooling sector [47].

Jinna Yu et al. (2021) [29] underscore the significance of renewable energy in the context of modern economic growth. Particularly, they emphasize the potential of solar-based renewable energy as an inexhaustible source that can effectively mitigate CO₂ emissions. However, prior empirical investigations have often overlooked this aspect. To address this gap, the researchers conducted a comprehensive study on the top 10 solar energy-consuming countries, including Australia, Germany, Japan, Spain, Italy, USA, South Korea, UK, France, and China. The study utilized a unique methodology known as 'Quantile-on-Quantile (QQ)' to analyze data spanning from 1991 to 2018.

The objective was to explore the asymmetric relationship between solar energy consumption and CO₂ emissions, thereby providing a robust framework to comprehend the interdependent structure between the two variables. The empirical findings revealed that, with the exception of France, solar energy usage contributed to a reduction in CO₂ emissions across various quantiles. Notably, the strength of this asymmetric link varied among countries, implying the need for cautious and attentive policy-making concerning solar energy and the environment. The research highlights the significance of incorporating solar energy in long-term growth strategies to improve environmental quality [48].

Taner Güney et al. (2021) [30] conducted a study that investigated the impact of solar energy and governance on CO₂ emissions using data from 35 countries with varying income levels from 2005 to 2018. The study revealed that solar energy adoption led to a decrease in CO₂ levels, as evidenced by estimates based on cross-section dependence and slope homogeneity. Moreover, the research identified governance as another influential factor, wherein the combination of solar energy expansion and effective governance contributed to CO₂ reduction. Thus, the authors recommend that governments prioritize solar energy adoption, considering its significant energy-generating potential, and simultaneously address governance issues to effectively curb CO₂ emissions [49].

The current research aims to examine the cooling effect of solar panels on temperatures and electrical efficiency using four distinct models for cooling. Specifically, the models include: 1) a solar panel with equal dimensions and a cooling fluid flowing through it, 2) the same model but with seven aluminum channels facilitating liquid flow, and 3) another version with nine channels for cooling fluid flow. In each model, water cooling and air cooling will be used, and the results will be compared with a reference plate without any cooling. Additionally, three different flow rates (0.35, 0.7, and 1.4 L/M) will be applied to all the models to investigate cooling differences accurately and comprehensively.

PART 3

NUMERICAL SIMULATION

3.1. INTRODUCTION

This section of our research focuses on providing a comprehensive numerical solution and mathematical formulation for heat transfer and fluid flow processes. The geometries of the involved systems were created using SolidWorks' software. To obtain the solutions, numerical methods are applied, and the continuity, momentum, and energy equations are solved using the ansys—22 programs. The implementation of turbulence models and finite volume techniques is also crucial in achieving accurate and efficient solutions within the fluid simulation system. This integrated approach allows us to gain valuable insights into the heat transfer and fluid behavior, contributing to a better understanding of the studied phenomena.

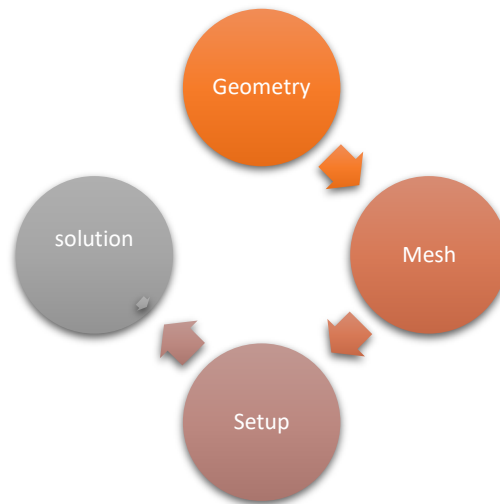


Figure 3.1. Ansys steps.

3.2. PHYSICAL MODEL

The physical model under investigation involves the study of cooling effects on a solar panel using channels through which water flows for cooling. The research entails two sets of experiments. In the first set, the solar panel will be cooled using water with varying flow rates of (0.35, 0.7, 1.4) L/M, and the resulting changes in temperature and electrical efficiency will be recorded. Subsequently, in the second set of experiments, the solar panel will be cooled again with water, but this time with flow rates of (0.35, 0.7, 1.4) L/M, and the temperatures and electrical efficiency will be measured and compared to the results obtained from the first set of experiments. By analyzing and contrasting the data from both sets of experiments, the study aims to understand the impact of cooling water flow rates on the solar panel's temperature and electrical efficiency. This investigation will provide valuable insights into optimizing the cooling system for enhanced performance and efficiency of the solar panel.

3.3. GEOMETRY DESIGN

The geometric shape of the solar panel and the channels required for the cooling fluid were designed using the SolidWorks 2020 software. This powerful CAD (Computer-Aided Design) program allowed for the creation of precise and detailed 3D models of the solar panel and the cooling channels, enabling a comprehensive representation of the system's physical structure. SolidWorks 2020 provided the necessary tools and features to accurately design and visualize the components involved in the study, facilitating the subsequent analysis and simulations of heat transfer and fluid flow processes. The utilization of SolidWorks 2020 ensured a robust and efficient approach to develop the physical model, which forms the basis for the numerical simulations and further investigations in this research.

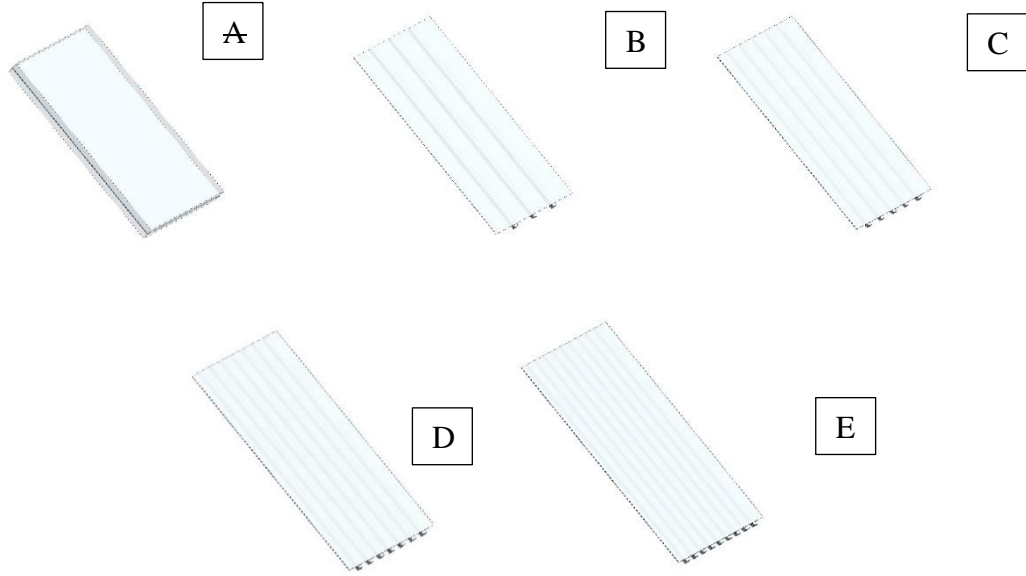


Figure 3.2. Geometry design a) For stander soler panel b) For 3 channel model c)For 5 channel model d) For 7 channel model e) For 9 channel model.

Table 3.1. The PV panel specifications.

Parameter	Value
Dimension of PV panel (L-W-H)	(1200-540-40) mm
The channel (L-W-H)	(120-2.54-2.54)cm
Max power	100 w
Voltage	22 volts
current	6.15mp

3.4. GOVERNING EQUATION

Mass conservation (the continuity equation):

$$\frac{\partial \bar{u}}{\partial x} + \frac{\partial \bar{v}}{\partial y} + \frac{\partial \bar{w}}{\partial z} = 0 \quad (3.1)$$

Momentum equation:

$$\left(\bar{u} \frac{\partial \bar{u}}{\partial x} + \bar{v} \frac{\partial \bar{u}}{\partial y} + \bar{w} \frac{\partial \bar{u}}{\partial z} \right) + \left(\frac{\partial}{\partial x} (\overline{u^2}) + \frac{\partial}{\partial y} (\overline{uv}) + \frac{\partial}{\partial z} (\overline{uw}) \right) = -\frac{1}{\rho} \frac{\partial \rho}{\partial x} + \frac{\mu}{\rho} \left(\frac{\partial^2 \bar{u}}{\partial x^2} + \frac{\partial^2 \bar{u}}{\partial y^2} + \frac{\partial^2 \bar{u}}{\partial z^2} \right) \quad (3.2)$$

$$\left(\bar{u} \frac{\partial \bar{v}}{\partial x} + \bar{v} \frac{\partial \bar{v}}{\partial y} + \bar{w} \frac{\partial \bar{v}}{\partial z} \right) + \left(\frac{\partial}{\partial x} (\overline{uv}) + \frac{\partial}{\partial y} (\overline{v^2}) + \frac{\partial}{\partial z} (\overline{uw}) \right) = -\frac{1}{\rho} \frac{\partial \rho}{\partial x} + \frac{\mu}{p} \left(\frac{\partial^2 \bar{v}}{\partial x^2} + \frac{\partial^2 \bar{v}}{\partial y^2} + \frac{\partial^2 \bar{v}}{\partial z^2} \right) \quad (3.3)$$

$$\begin{aligned} & \left(\bar{u} \frac{\partial \bar{w}}{\partial x} + \bar{v} \frac{\partial \bar{w}}{\partial y} + \bar{w} \frac{\partial \bar{w}}{\partial z} \right) + \left(\frac{\partial}{\partial x} (\overline{uw}) + \frac{\partial}{\partial y} (\overline{vw}) + \frac{\partial}{\partial z} (\overline{w^2}) \right) \\ & = -\frac{1}{\rho} \frac{\partial \rho}{\partial x} \frac{\mu}{p} \left(\frac{\partial^2 \bar{w}}{\partial x^2} + \frac{\partial^2 \bar{w}}{\partial y^2} + \frac{\partial^2 \bar{w}}{\partial z^2} \right) \end{aligned} \quad (3.4)$$

Energy equation:

$$\left(\bar{u} \frac{\partial \bar{T}}{\partial x} + \bar{v} \frac{\partial \bar{T}}{\partial y} + \bar{w} \frac{\partial \bar{T}}{\partial z} \right) + \left(\frac{\partial}{\partial x} (\overline{uT}) + \frac{\partial}{\partial y} (\overline{vT}) + \frac{\partial}{\partial z} (\overline{wT}) \right) = \alpha \left(\frac{\partial^2 \bar{T}}{\partial x^2} + \frac{\partial^2 \bar{T}}{\partial y^2} + \frac{\partial^2 \bar{T}}{\partial z^2} \right) \quad (3.5)$$

In the context of the exact k-epsilon equations for turbulence modeling, various terms remain unknown and unmeasurable. To address this complexity and make the approach more practical, the traditional k-epsilon turbulence model, as proposed by Launder and Spalding, is employed. This choice is based on our current best understanding of the underlying turbulent processes, which helps to reduce ambiguity in the modeling approach. By utilizing the k-epsilon turbulence model, a set of equations is presented that can be applied effectively across a wide range of turbulent applications. This model offers a practical and reliable solution for turbulent flow simulations, considering the limitations and challenges associated with directly solving the exact k-epsilon equations in real-world scenarios.

In terms of turbulent kinetic energy

$$\frac{\partial}{\partial t} (\rho k) + \frac{\partial (\rho k u_i)}{\partial x_i} = \frac{\partial}{\partial x_j} \left[\frac{\mu_t}{\rho k} \frac{\partial k}{\partial x_j} \right] + 2\mu^t E_{ij} E_{ij} - \rho \epsilon \quad [50] \quad (3.6)$$

Dissipation Rate Equation:

$$\rho \left(\bar{u} \frac{\partial \epsilon}{\partial x} + \bar{v} \frac{\partial \epsilon}{\partial y} + \bar{w} \frac{\partial \epsilon}{\partial z} \right) \left[\left(\mu + \frac{\mu_t}{\sigma_{\epsilon\epsilon}} \right) \cdot \left(\frac{\partial^2 \epsilon}{\partial x^2} + \frac{\partial^2 \epsilon}{\partial y^2} + \frac{\partial^2 \epsilon}{\partial z^2} \right) \right] + C_{1\epsilon} \frac{\epsilon}{k} G_k - C_{2\epsilon} \rho \frac{\epsilon}{k} \quad (3.7)$$

Eddy viscosity of turbulent

$$\mu_t = \rho C_p \frac{k^2}{\epsilon} \quad [51] \quad (3.8)$$

To calculate the Electrical efficiency by this equation:

$$\eta_{el} = \eta_{ref} \left(1 - \gamma (T_c - T_{ref}) \right) \quad (3.9)$$

where η_{ref} Is the reference efficiency of the PV module ($\eta_{ref} = 0.12$); γ is a temperature coefficient ($\gamma = 0.0045 \text{ } ^\circ\text{C}^{-1}$), T_c Is the cell temperature and T_{ref} Is the reference temperature (25°C, optimum operating temperature of PV modules at the rated power).[52]

3.5. MESH GENERATION

To obtain accurate results, a precisely detailed network of the engineering body must be created to draw more accurate results in the ansys procedures.

Details of "Mesh"	
Display	
Display Style	Use Geometry Setting
Defaults	
Physics Preference	CFD
Solver Preference	Fluent
Element Order	Linear
<input type="checkbox"/> Element Size	5.0 mm
Export Format	Standard
Export Preview Surface Mesh	No
Sizing	
Use Adaptive Sizing	No
<input type="checkbox"/> Growth Rate	Default (1.2)
<input type="checkbox"/> Max Size	5.0 mm
Mesh Defeaturing	Yes
<input type="checkbox"/> Defeature Size	Default (2.5e-002 mm)
Capture Curvature	Yes
<input type="checkbox"/> Curvature Min Size	Default (5.e-002 mm)
<input type="checkbox"/> Curvature Normal Angle	Default (18.0°)
Capture Proximity	No
Bounding Box Diagonal	1383.6 mm
Average Surface Area	56051 mm ²
Minimum Edge Length	0.5 mm
Quality	
Inflation	
Advanced	
Statistics	
<input type="checkbox"/> Nodes	1027142
<input type="checkbox"/> Elements	979200

Figure 3.3. Details of mesh in ansys.22.

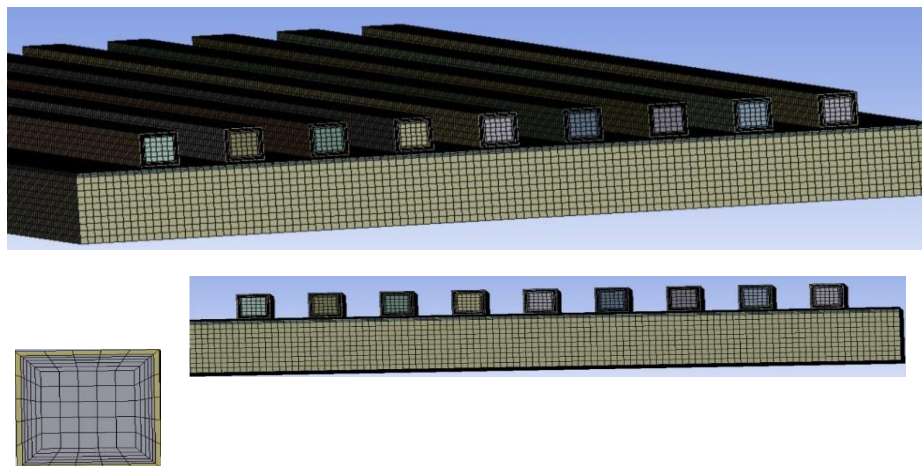


Figure 3.4. form of mesh

3.6. SETUP

Upon configuring the network based on the designated geometry, essential parameters and their respective values are incorporated into the study to facilitate data extraction. These parameters include input temperatures, flow rates, as well as material and fluid

properties. To ensure heightened precision and enable a comprehensive investigation, the study adopts transient simulation techniques. By employing transient simulation, the obtained results are expected to be more accurate and offer a deeper understanding of the phenomenon under examination.

The image shows a software dialog box titled "Mass-Flow Inlet". At the top, there is a "Zone Name" field containing the text "inlet". Below this is a horizontal menu with tabs for "Momentum", "Thermal", "Radiation", "Species", "DPM", "Multiphase", "Potential", "Structure", and "UDS". The "Momentum" tab is currently selected. The main area contains several configuration options:

- Reference Frame: Absolute
- Mass Flow Specification Method: Mass Flow Rate
- Mass Flow Rate [kg/s]: 0.01166
- Supersonic/Initial Gauge Pressure [Pa]: 0
- Direction Specification Method: Normal to Boundary

Below these options is a section titled "Turbulence" with the following settings:

- Specification Method: Intensity and Viscosity Ratio
- Turbulent Intensity [%]: 5
- Turbulent Viscosity Ratio: 10

At the bottom of the dialog are three buttons: "Apply", "Close", and "Help".

Figure 3.5. Mass-flow inlet in setup.

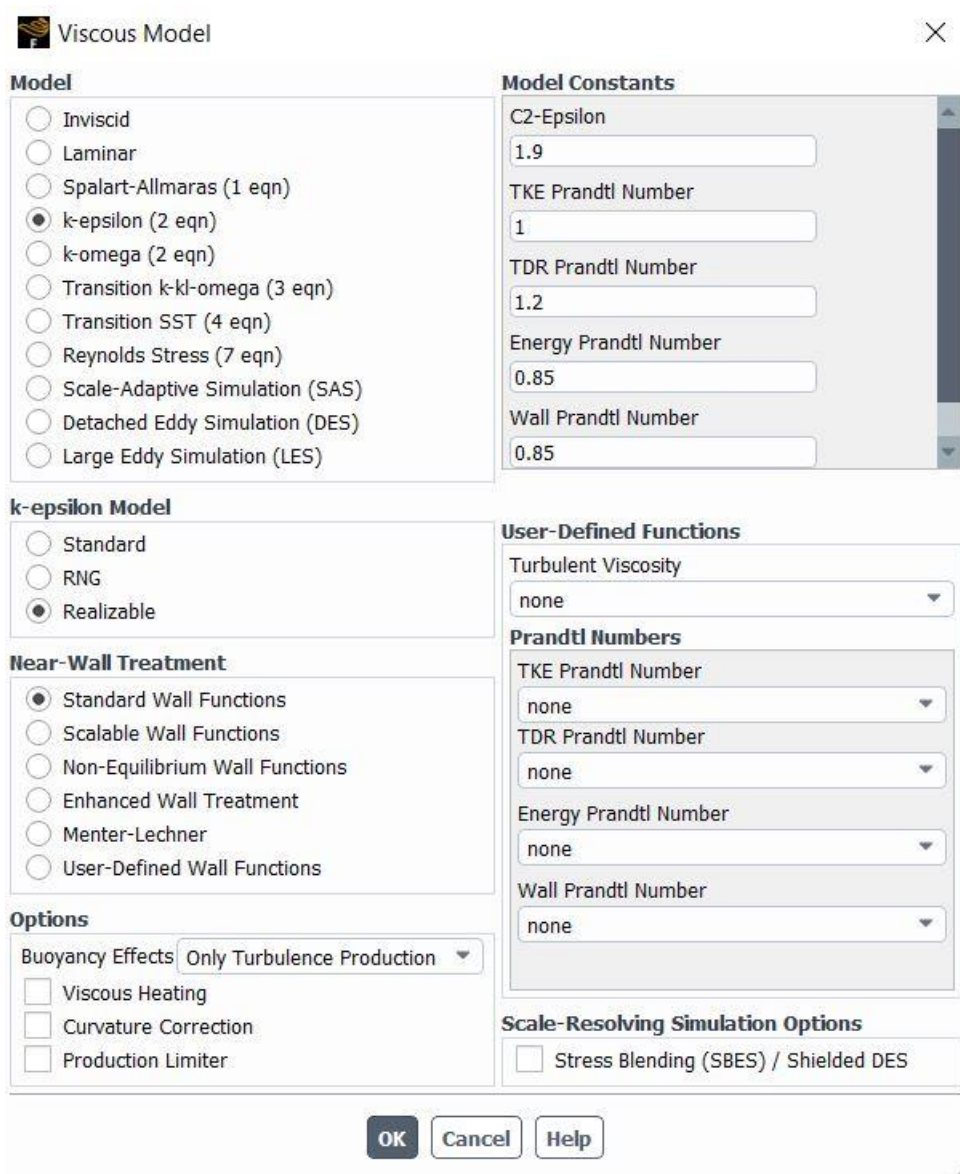


Figure 3.6. Viscous model in setup.

3.7. BOUNDARY CONDITIONS

Table 3.2. Inlet boundary conditions.

Inlet temperature	25 C
Flowrate	(0.35,0.7,1.4) L/M
Turbulent intensity	5%

PART 4

RESULTS AND DISCUSSION

4.1. GENERAL

This chapter presents the theoretical and computational outcomes of cooling solar panels using the Ansys.22 program. The cooling methods considered involve water and air, implemented through channels with specific flow rates (0.35, 0.7, 1.4 L/m). The study investigates four different models, denoted as Models Five, Seven, and Nine, while also conducting a comparison between them. Additionally, the type of cooling liquid utilized is assessed, and the temperature distribution across the solar panel is analyzed. Furthermore, the electric efficiency for each cooling scenario is calculated.

The average temperature is determined using CFD-post within the Ansys results. This involves the utilization of contours or the Function Calculator, where the "Area Ave" function is employed to accurately calculate temperature at specified locations on the solar panel, ensuring precise temperature distribution analysis.

To account for radiation effects, the Radiation Model is employed in conjunction with the Solar Calculator. Careful selection of inputs, including the solar panel's direction, location, date, and time, enables the calculation of radiation incident on the solar panel over an eight-hour period, commencing from 7:00 am to 3:00 pm, as illustrated in the figure below.

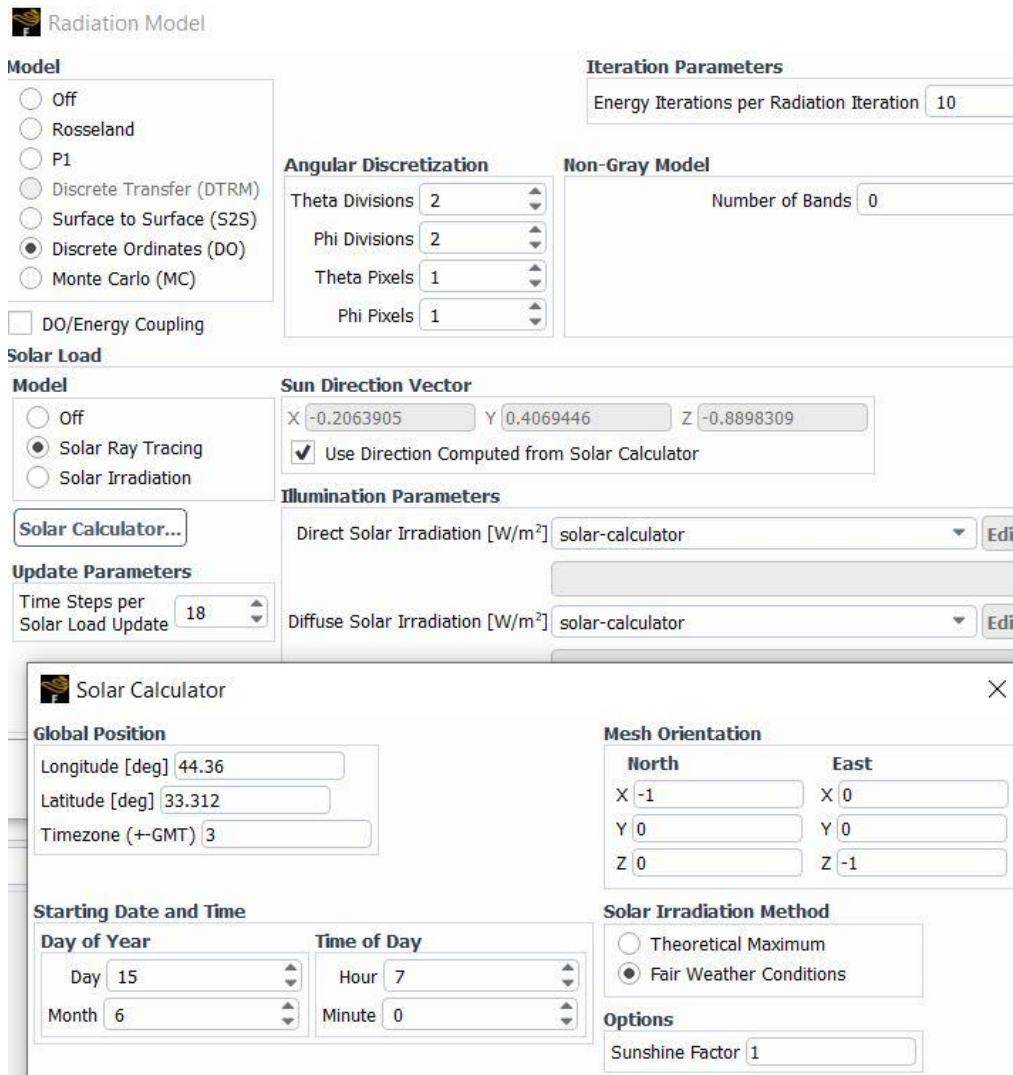


Figure 4.1. Details of Radiation Model.

4.2. SOLER PANEL REFERENCE

Figure 4.3 illustrates the temperature distribution within the uncooled solar panel, revealing a notable increase in temperature over time. The plate temperature steadily rises and reaches its peak at 18700 seconds (corresponding to 12:11 pm). Subsequently, the plate temperature exhibits a gradual decline.

In Figure 4.4, a remarkable reduction in the electrical efficiency of the solar panel is observed as the temperature increases, eventually reaching its maximum value. The electrical efficiency plummets to its lowest point due to the elevated temperature of the solar panel. However, as the solar panel's temperature begins to decrease, the

electrical efficiency slightly improves. Notably, the least efficient point corresponds to the highest temperature of the solar cell, which is recorded at 9.44905%.

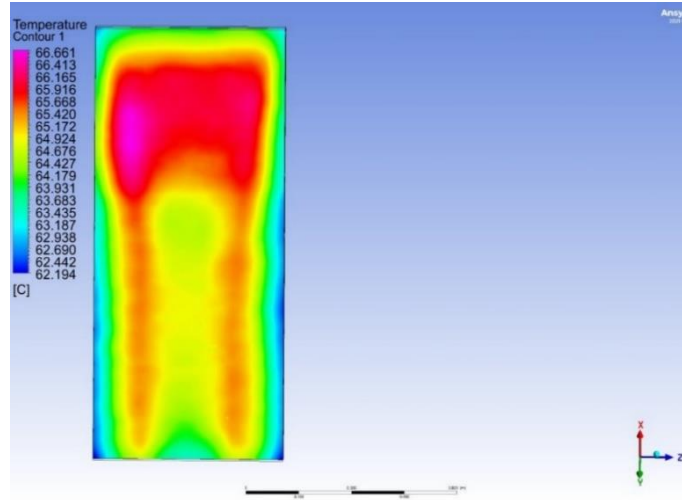


Figure 4.2. Temperature distribution of the solar panel reference.

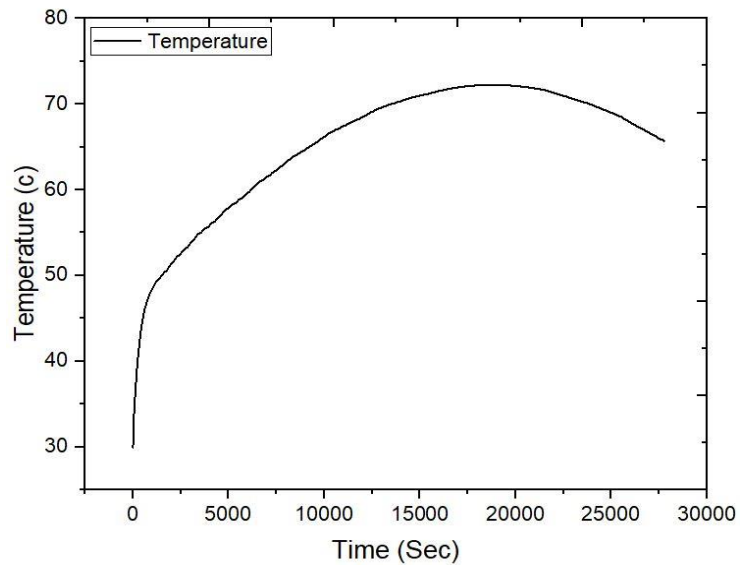


Figure 4.3. Temperature changes with time for the reference panel.

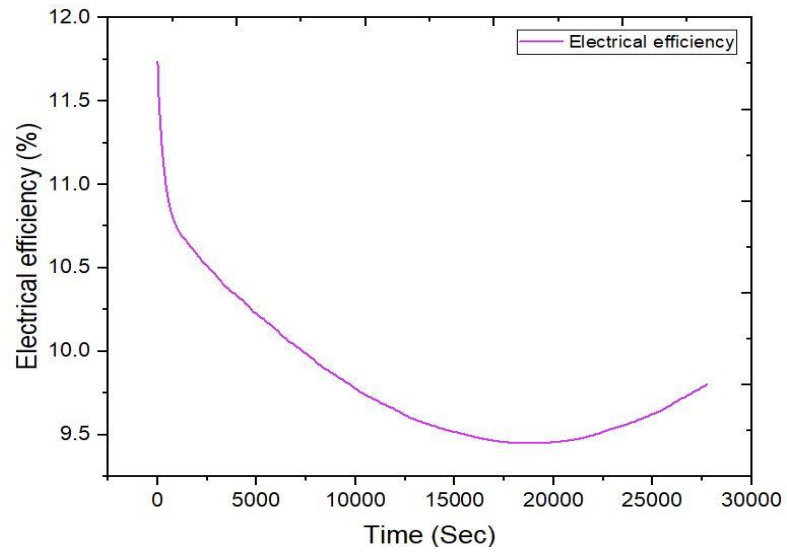


Figure 4.4. Change of electrical efficiency with time for the reference panel.

4.3. WATER COOLING SYSTEM

4.3.1. Three Channel Model

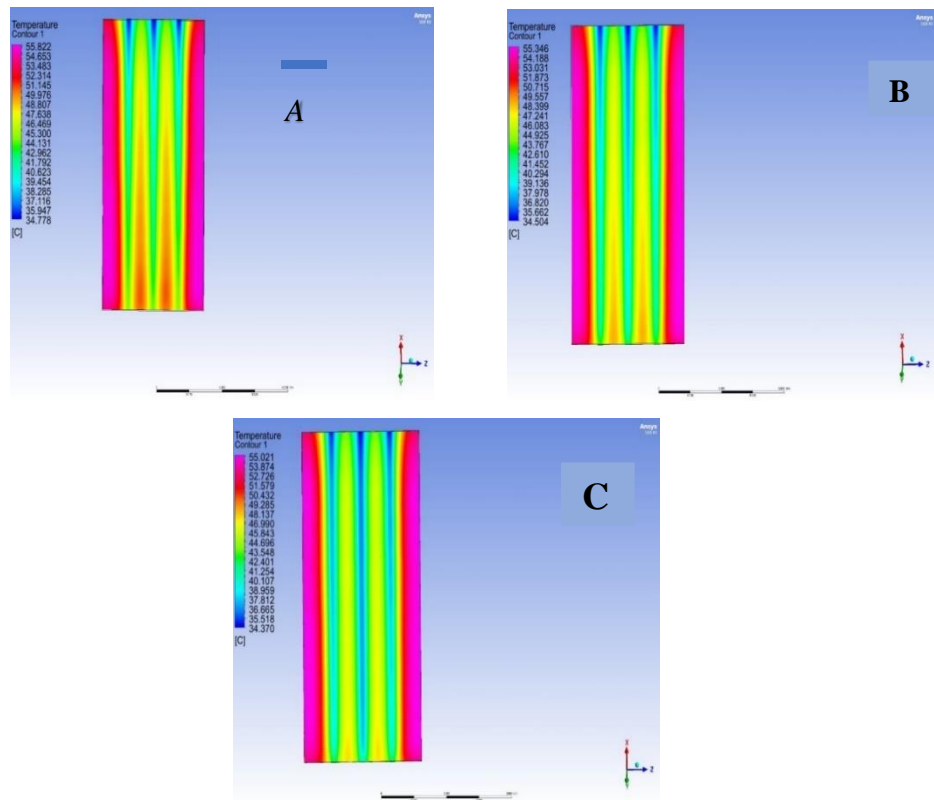


Figure 4.5. Temperature distribution on the solar panel in 3 channel A)for 0.35L/M, B)for 0.7L/M, C)for 1.4L/M.

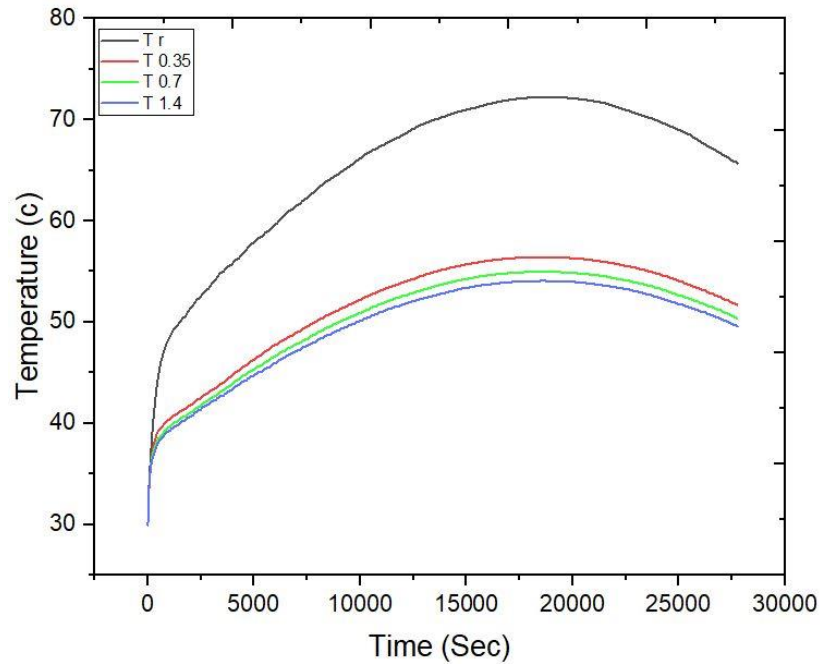


Figure 4.6. Temperature changes with time in the solar panel at three-channel water cooling.

Figure 4.6 demonstrates the impact of cooling on maintaining the temperature of the solar panel in comparison to the non-cooled reference. Initially, the curve shows an upward trend, with the highest temperature recorded at 18700 seconds (12:11 pm), reaching 72.23°C in the non-cooled reference case. However, when applying cooling with a flow rate of 0.35 L/M, the highest temperature drops to 56.42°C. Further cooling with a flow rate of 0.7 L/M results in a reduction of the highest temperature to 54.97°C, while the most effective cooling occurs with a flow rate of 1.4 L/M, resulting in the lowest highest temperature of 52.04°C.

Subsequently, the curve gradually descends as the temperature of the solar panel decreases. It is evident that the most efficient cooling is achieved when the flow rate is set to 1.4 L/M, and the cooling effectiveness diminishes with reduced flow rates, when compared with the reference panel without any cooling measures.

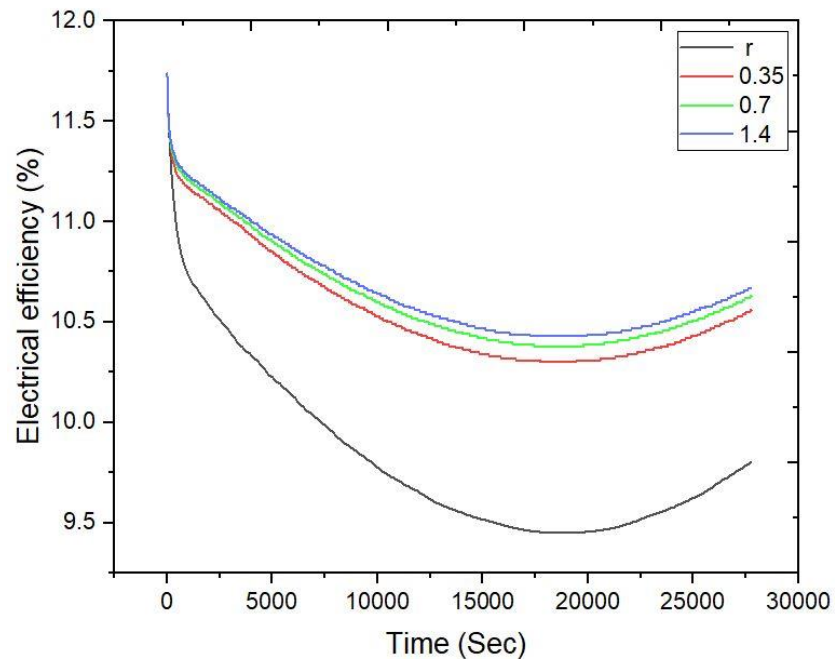


Figure 4.7. Electrical efficiency changes with time three channel water cooling

Figure 4.7 depicts the variation in electrical efficiency resulting from the disparities in the solar panel's temperature. The efficiency demonstrates a gradual decline, reaching its lowest point at 18700 seconds (12:11 pm) in the reference panel without any cooling measures, registering at 9.44%. However, when cooling is applied with a flow rate of 0.35 L/M, the efficiency improves to 10.3%. Further enhancement in efficiency is observed when cooling with a flow rate of 0.7 L/M, reaching 10.38%. Remarkably, the highest efficiency is achieved when the cooling flow rate is set to 1.4 L/M, reaching 10.43%.

It is evident that a higher flow rate yields superior cooling efficiency for the solar panel when compared to the reference panel without any cooling intervention.

4.3.2. Five Channel Model

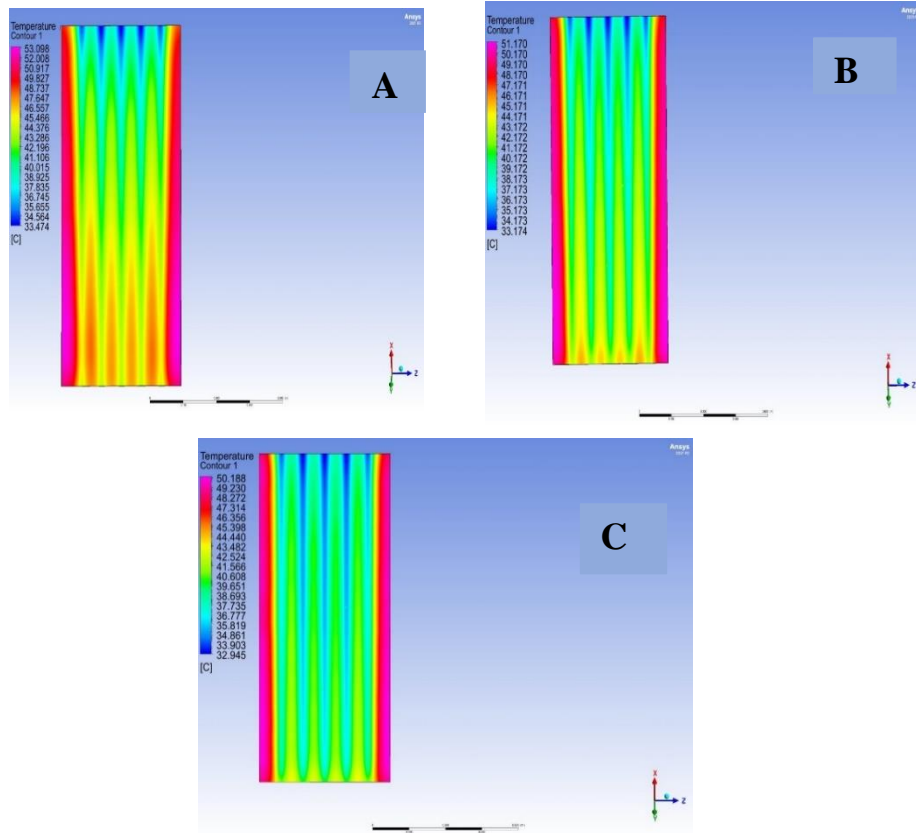


Figure 4.8. Temperature distribution on the solar panel in 5 channel a) for 0.35L/M, b) for 0.7L/M, c) for 1.4L/M.

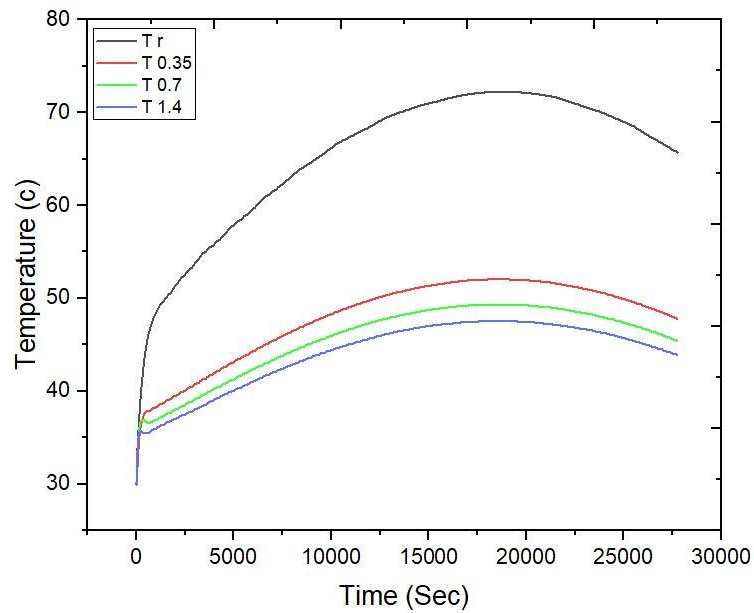


Figure 4.9. The temporal variation of temperature in the solar panel with a five-channel water cooling system.

Figure 4.9 illustrates the impact of cooling on maintaining the temperature of the solar panel as compared to a non-cooled scenario. The temperature curve shows an upward trend until it reaches its peak at 18700 seconds (12:11 pm), with the reference temperature recorded as 72.23°C.

Upon implementing cooling, at a flow rate of 0.35 L/M, the temperature is reduced to 52.04°C, and with a higher flow rate of 0.7 L/M, the temperature further decreases to 49.33°C. The most effective cooling is achieved with a flow rate of 1.4 L/M, which results in the lowest temperature of 47.54°C. Beyond this point, the curve exhibits a gradual decline due to the continuous decrease in the solar panel's temperature.

Comparing these results with the reference plate, it is evident that the cooling system is successful in maintaining lower temperatures. Notably, reducing the flow rate leads to a diminished cooling effect.

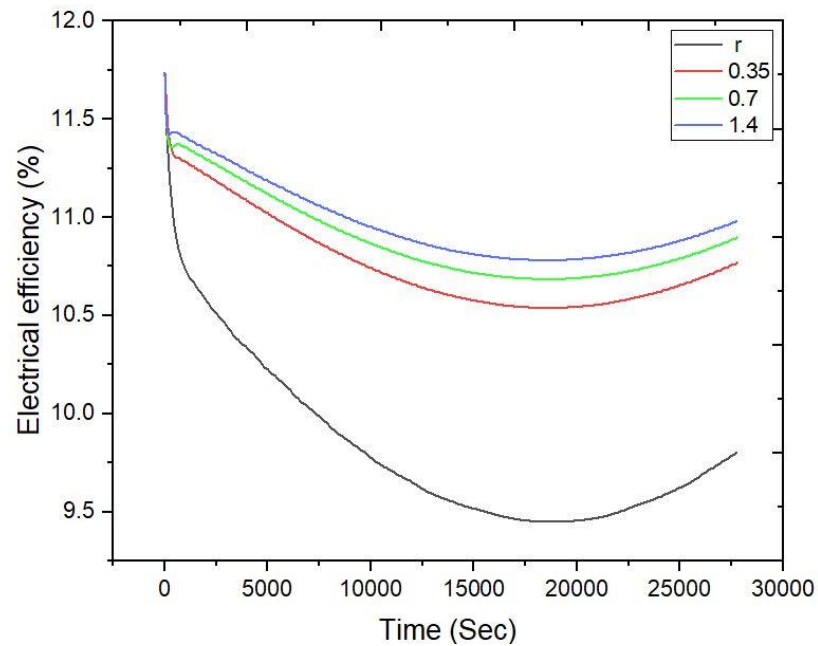


Figure 4.10. The electrical efficiency of a five-channel water cooling system varies over time.

Figure 4.10 illustrates the impact of solar panel temperature variation on electrical efficiency. The efficiency of the solar panel gradually declines until it reaches its lowest point at 18,700 seconds (12:11 pm) in the reference panel without any cooling,

measuring at 9.44%. Conversely, when the panel is cooled with a flow rate of 0.35 L/M, the efficiency increases to 10.53%, and with a flow rate of 0.7 L/M, it further improves to 10.68%. Employing a higher flow rate of 1.4 L/M yields the highest efficiency at 10.78%. Notably, greater flow rates result in superior cooling efficiency for the solar panel compared to the reference panel.

4.3.3. Seven Channel Model

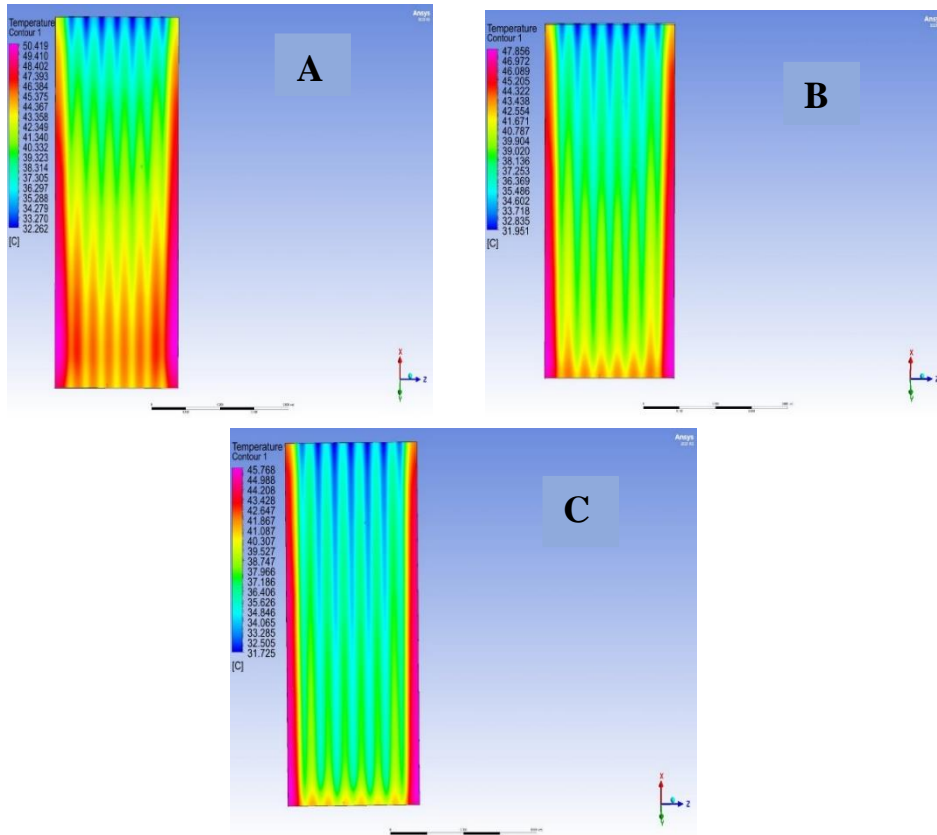


Figure 4.11. Temperature Distribution on the Solar Panel Across Different Flow Rates in Seven Channels A) for 0.35L/M, b) for 0.7L/M, c) for 1.4L/M.

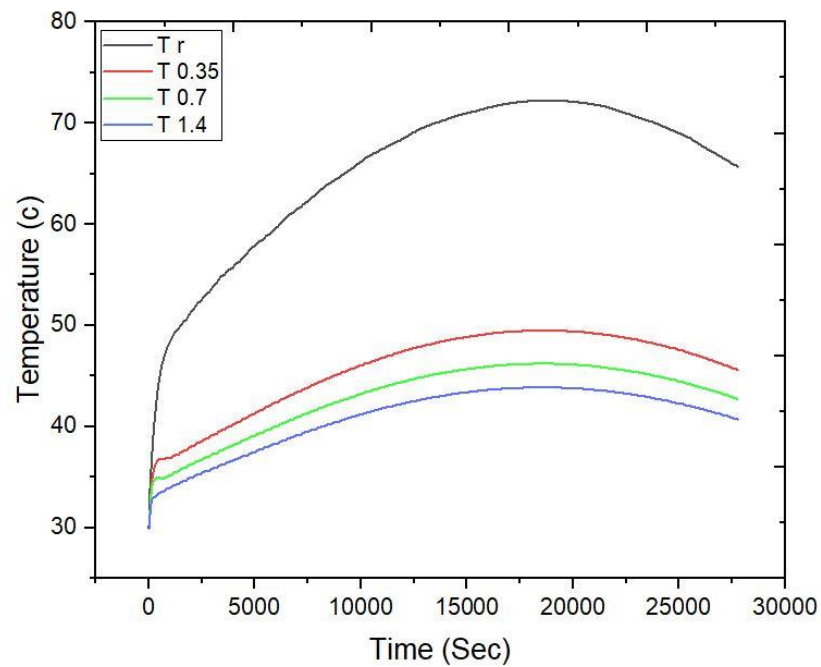


Figure 4.12. Temperature Variation over Time in a Three-Channel Water-Cooled Solar Panel.

Figure 4.12 shows the effect of cooling on keeping the solar panel's temperature compared to the forum without cooling. The curve rises until the highest temperature reaches 18700 seconds (12:11 pm) when the reference is 72.23C. Still, when cooling, the flow (0.35 L/M) is 49.50 C. When cooling with a flow of (0.7 L/M), the highest temperature is 46.21 C. When cooling with a flow of (1.4 L/M), the highest temperature is 43.87 C. After that; the curve begins to descend gradually due to the solar panel's temperature decrease. The best cooling is when the flow is (1.4 L/M), and the cooling decreases when the flow is reduced. Compared with the reference plate

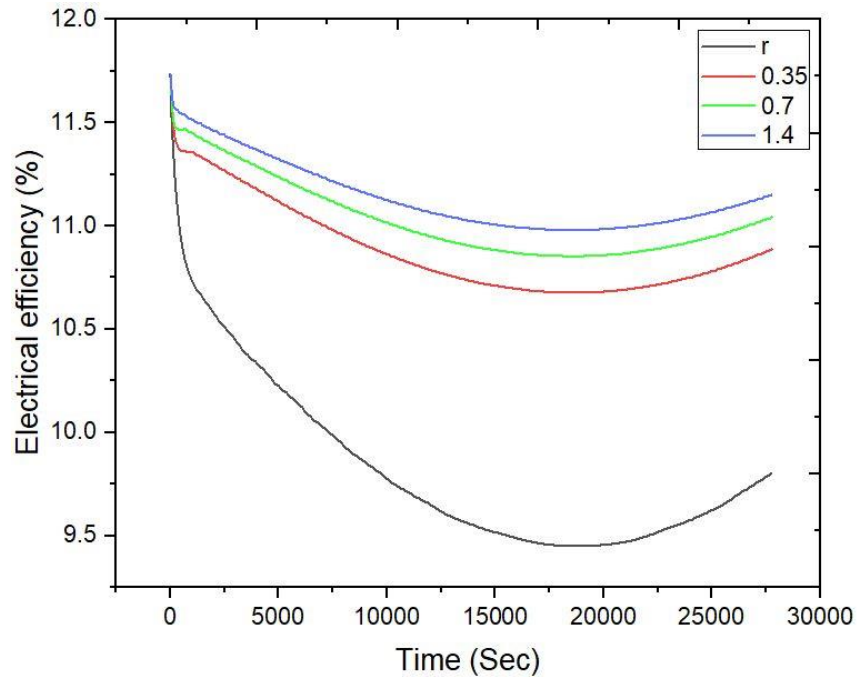


Figure 4.13. Electrical efficiency changes with time seven channel water cooling.

Figure 4.12 illustrates the impact of cooling on maintaining the temperature of the solar panel, in comparison to the scenario without any cooling mechanism. Initially, the temperature curve exhibits an ascending trend until it reaches its peak at 18700 seconds (12:11 pm), with the reference temperature recorded at 72.23°C. However, when cooling is applied with a flow rate of 0.35 L/M, the temperature reduces to 49.50°C. Further enhancing the cooling process with a flow rate of 0.7 L/M leads to a decrease in the highest temperature to 46.21°C. The most efficient cooling is achieved at a flow rate of 1.4 L/M, which results in the lowest peak temperature of 43.87°C. Subsequently, the temperature curve begins to gradually decline as the solar panel's temperature decreases. It is evident that the optimal cooling performance is observed at a flow rate of 1.4 L/M, and cooling efficiency diminishes with the reduction in flow rate. A comparative analysis with the reference plate supports these findings.

4.3.4. Nine Channel Model

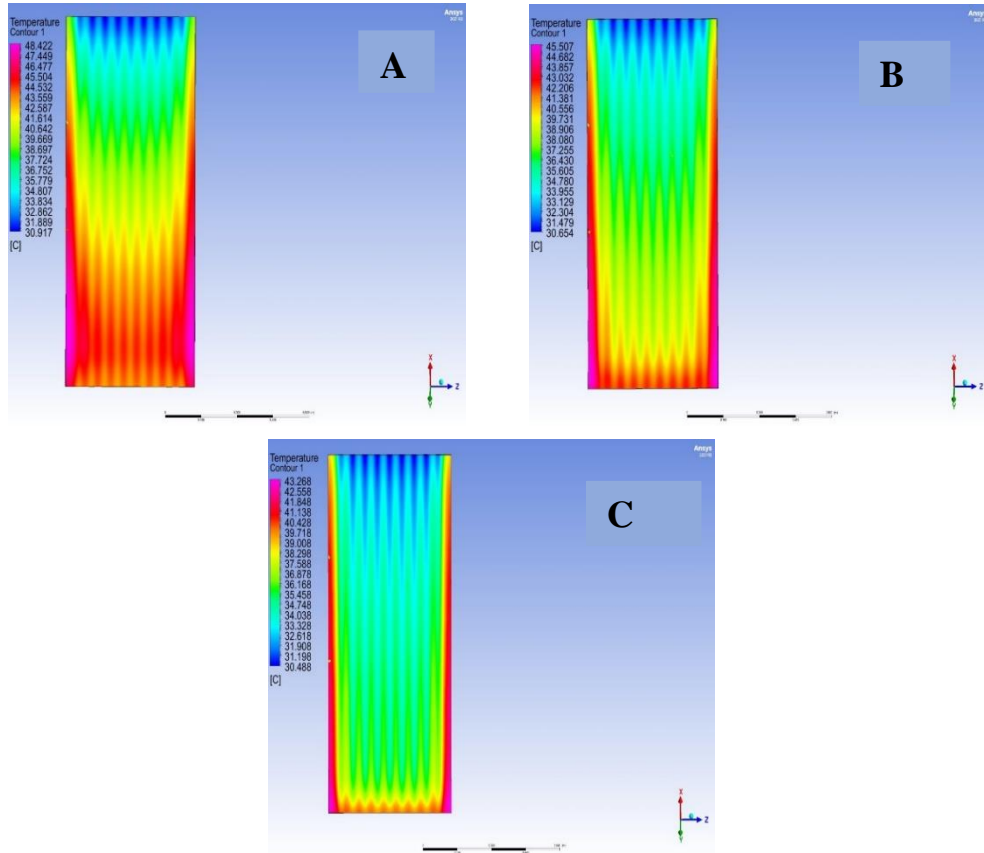


Figure 4.14. Temperature Distribution Across Nine Channels on the Solar Panel a) for 0.35L/M, b) for 0.7L/M, c) for 1.4L/M.

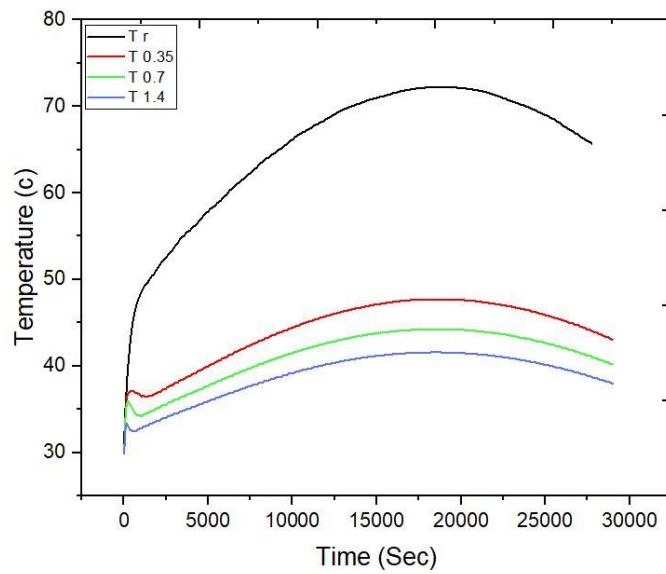


Figure 4.15. Temporal Variation of Solar Panel Temperature with Nine-Channel Water Cooling

Figure 4.15 illustrates the impact of water cooling on the temperature regulation of a solar panel when compared to an uncooled control. The temperature curve exhibits an upward trend until it reaches its peak at 18700 seconds (12:11 pm) with a reference temperature of 72.23°C. Conversely, under the influence of cooling, the temperature remains at 47.71°C when the flow rate is set at 0.35 L/M. With an increased flow rate of 0.7 L/M, the highest temperature drops to 44.25°C, and further decreases to 41.58°C when the flow rate is set at 1.4 L/M. Subsequently, the curve demonstrates a gradual descent, indicative of the solar panel's cooling effect. Notably, the optimal cooling performance is achieved at a flow rate of 1.4 L/M, while a reduction in flow rate leads to a diminished cooling effect compared to the reference panel.

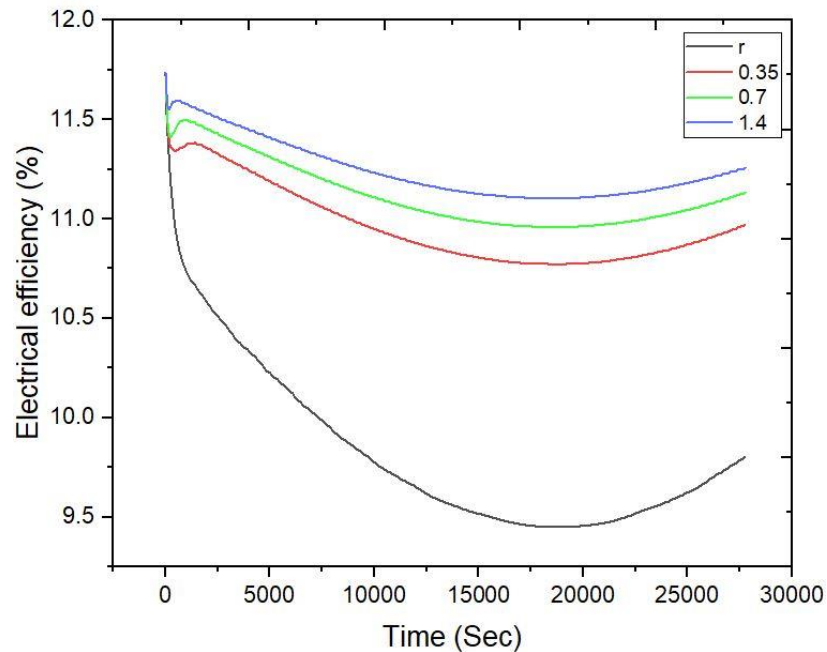


Figure 4.16. Temporal Variation of Electrical Efficiency in Nine-Channel Water Cooling System.

Figure 4.16 illustrates the temporal changes in electrical efficiency resulting from variations in the solar panel's temperature in a nine-channel water cooling system. The efficiency exhibits a gradual decline, reaching its minimum value at 18700 seconds (12:11 pm) for the reference panel without any cooling, registering at 9.44%. Conversely, when subjected to cooling with a flow rate of 0.35 L/min, the efficiency improves to 10.77%. Further enhancement is observed when the cooling flow rate is increased to 0.7 L/min, yielding an efficiency of 10.96%. The highest efficiency of

11.10% is achieved with a cooling flow rate of 1.4 L/min. These findings demonstrate that increased flow rates lead to superior cooling efficiency for the solar panel compared to the reference panel without any cooling mechanism.

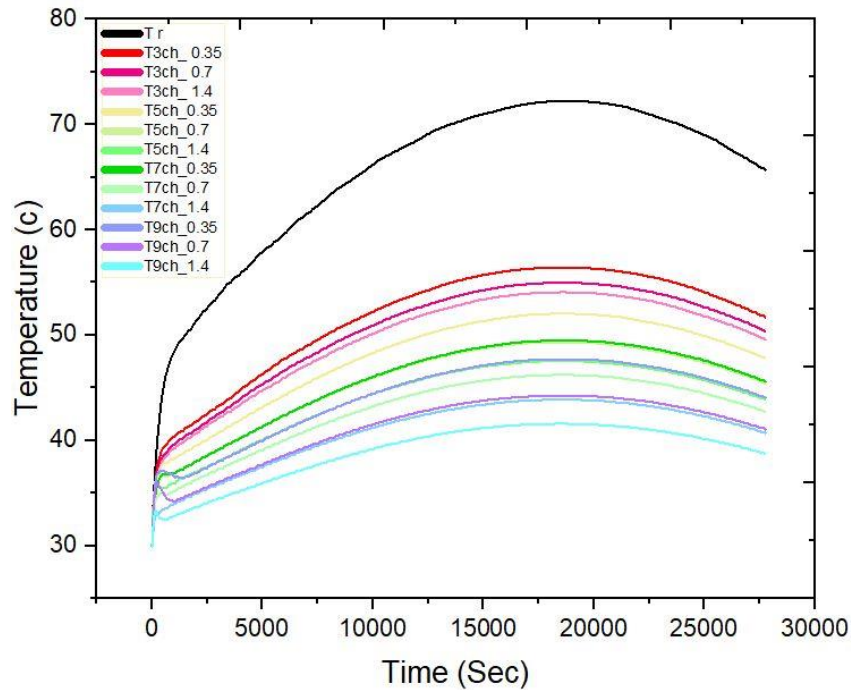


Figure 4.17. Temperature Variation over Time in Solar Panels with Water-Cooling Channels.

The results demonstrate that the implementation of cooling mechanisms effectively reduces the operating temperature of the solar panels. Among the tested configurations, the 9-channel model exhibits the most favorable cooling outcomes, followed by the 7-channel model, the 5-channel model, and lastly, the 3-channel model, when compared to the reference panel without any cooling mechanism. It is worth noting that an increase in the number of channels correlates with improved cooling performance, resulting in reduced solar panel temperatures.

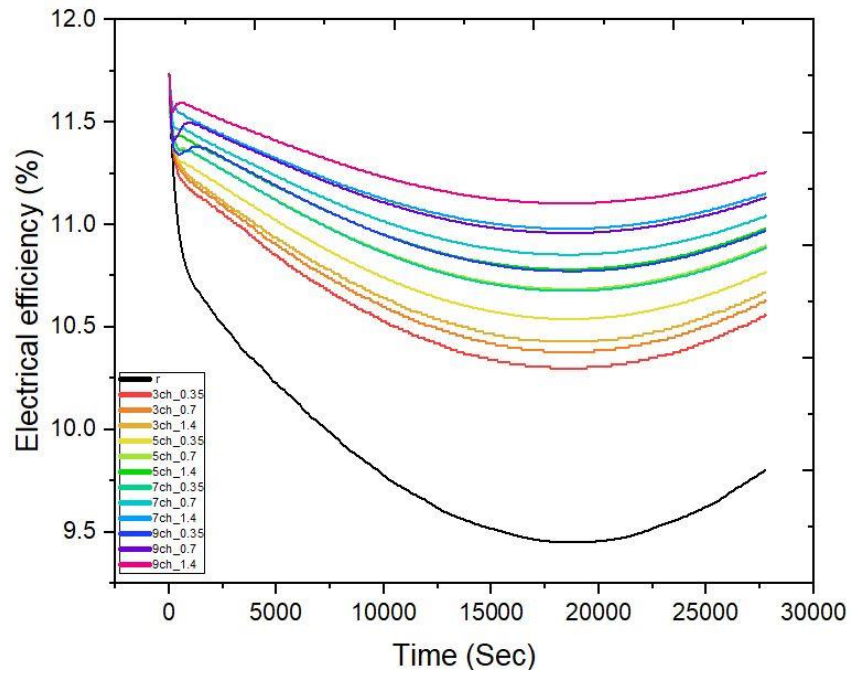


Figure 4.18. Time-Dependent Variation of Electrical Efficiency in Water-Cooled Solar Panels.

The electrical efficiency of the reference panel, operating without cooling, is found to be lower compared to the solar panel with an active cooling system. Notably, the introduction of cooling leads to variations in electrical efficiency over time, with different channel configurations showing distinct performance levels. Among the investigated models, the 9-channel configuration exhibits the highest electrical efficiency, followed by the 7-channel model, the 5-channel model, and lastly, the 3-channel model. This observed trend can be attributed to the impact of temperature changes on the solar panel's overall performance.

4.4. AIR COOLING SYSTEM

4.4.1. Three Channel Model

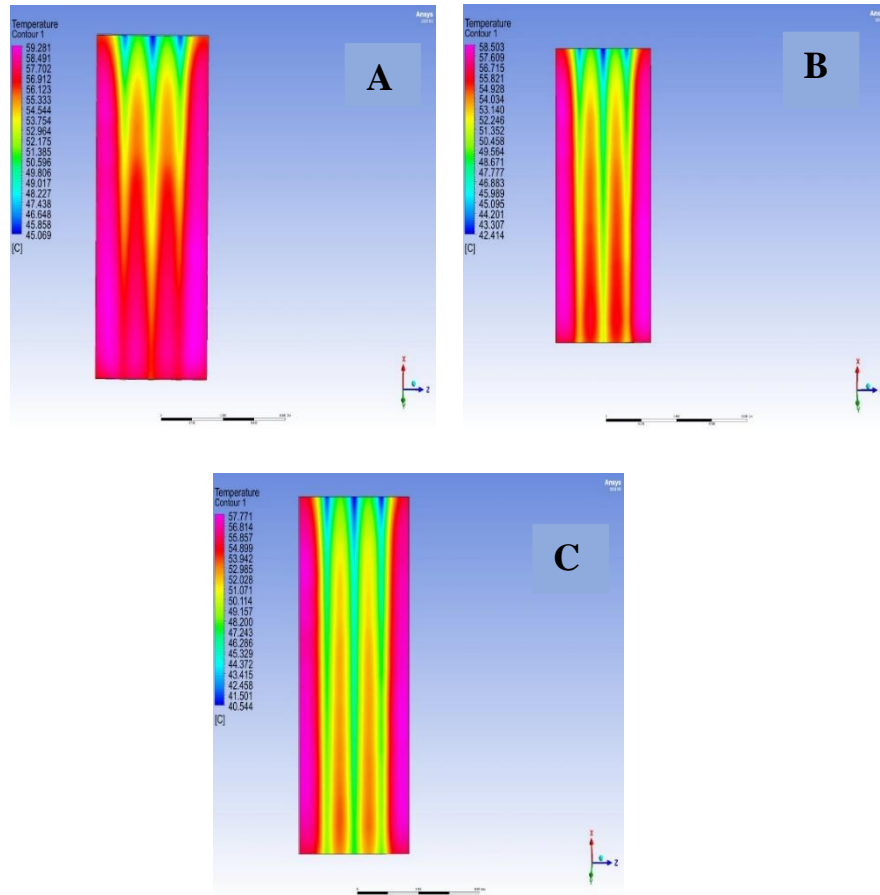


Figure 4.19. Temperature distribution on a solar panel under three-channel air cooling conditions. a) for 0.35L/M, b) for 0.7L/M, c) for 1.4L/M.

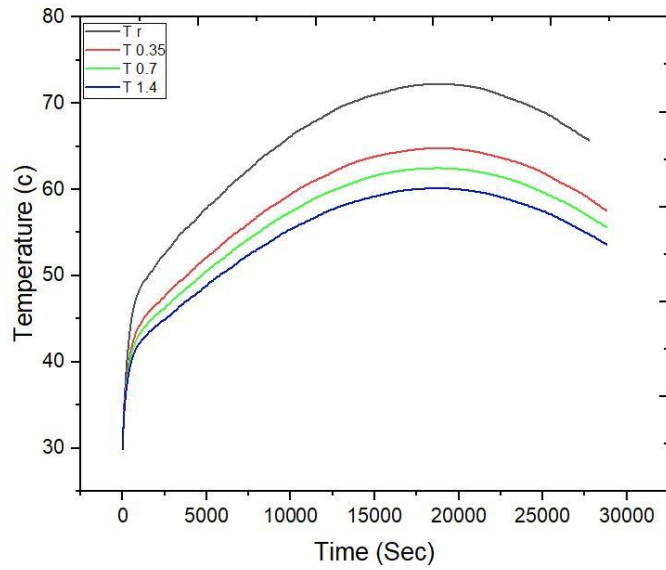


Figure 4.20. Temporal variation of temperature in a solar panel under three-channel air cooling conditions.

The graph depicts the impact of cooling on the solar panel's temperature compared to an uncooled board. Initially, the temperature curve ascends until it reaches its peak at 18700 seconds (12:11 pm), with the reference panel recording a temperature of 72.23°C. In contrast, the cooled panel with a flow rate of 0.35 L/M exhibits a temperature of 64.80°C, and when the flow rate is increased to 0.7 L/M, the temperature drops to 62.48°C. The most efficient cooling is observed with a flow rate of 1.4 L/M, resulting in the lowest temperature of 60.14°C. Subsequently, the temperature gradually decreases due to continuous cooling of the solar panel. Notably, the highest cooling efficiency is achieved at a flow rate of 1.4 L/M, and cooling

effectiveness diminishes with reduced flow rates. A comparison with the reference panel highlights the benefits of employing the three-channel air cooling method.

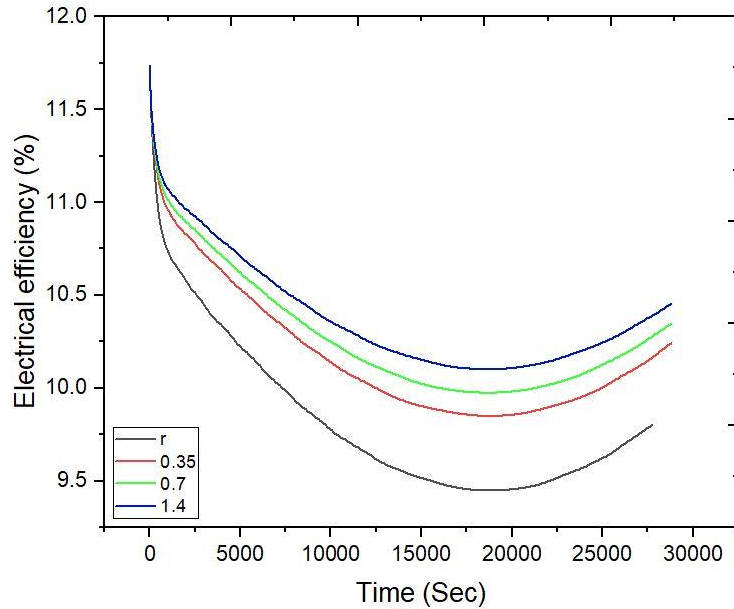


Figure 4.21. Variation in Electrical Efficiency with three-Channel Air Cooling.

Figure 4.21 depicts the variation in electrical efficiency concerning the solar panel's temperature under three-channel air cooling conditions. The graph showcases a gradual decrease in electrical efficiency, reaching its lowest value at 18700 seconds (12:11 pm) for the uncooled reference panel, measuring 9.44%. However, with cooling, the electrical efficiency improves to 9.85% for a flow rate of 0.35 L/M, 9.97% for a flow rate of 0.7 L/M, and 10.10% for a flow rate of 1.4 L/M. These results indicate that higher flow rates contribute to enhanced cooling efficiency of the solar panel compared to the uncooled reference panel.

4.4.2. Five Channel Model

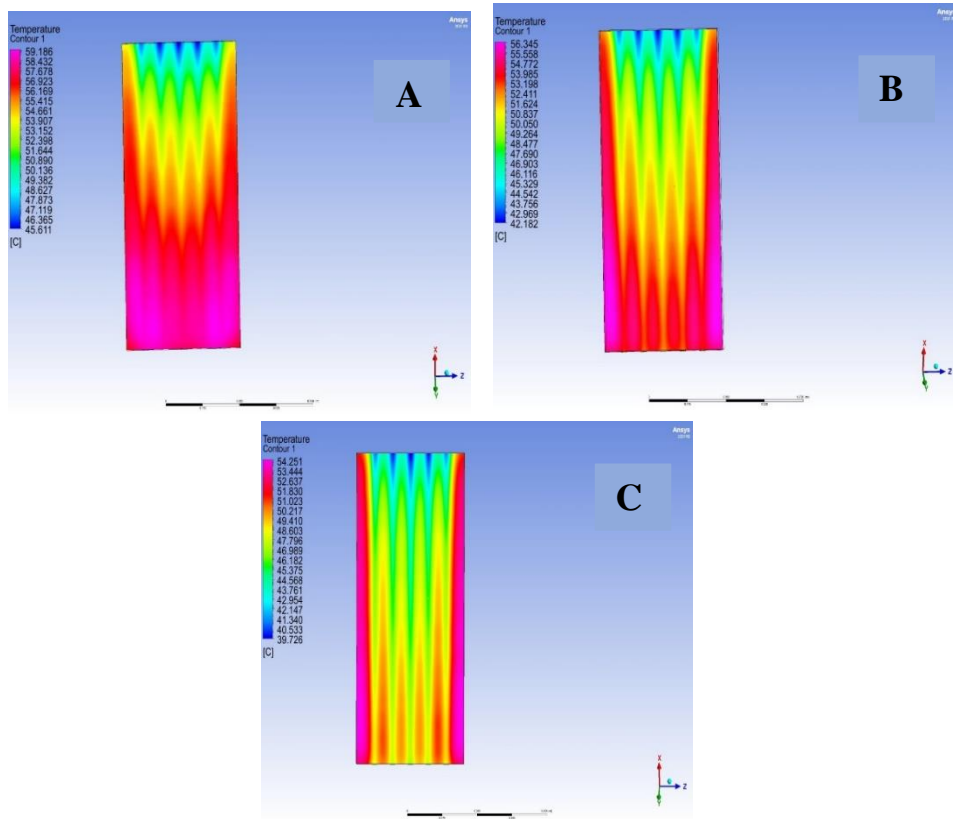


Figure 4.22. Temperature distribution on the solar panel utilizing a five-channel cooling system. a) for 0.35L/M, b) for 0.7L/M, c) for 1.4L/M.

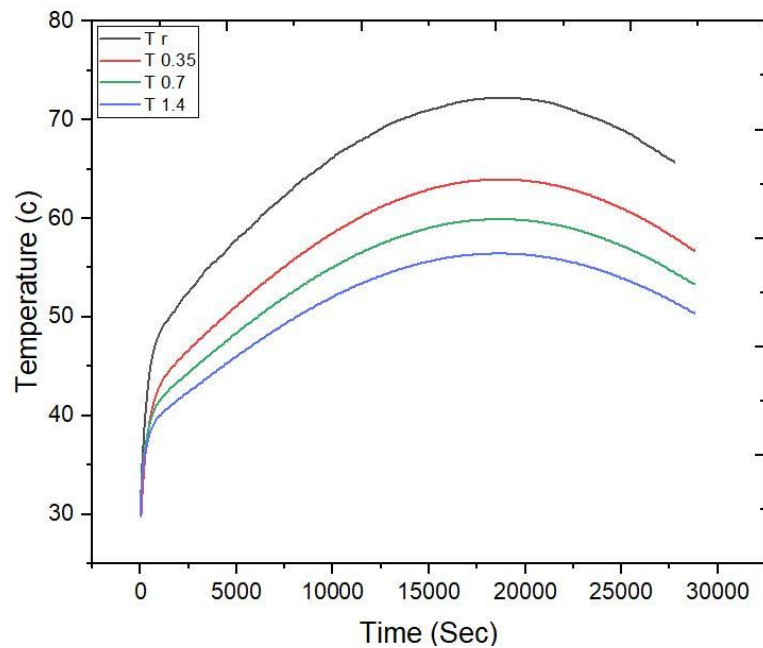


Figure 4.23. Variations in temperature over time on the solar panel subjected to air cooling through the five-channel configuration.

Figure 0.1 showcases the impact of cooling on maintaining the solar panel's temperature in comparison to the scenario without any cooling. The temperature curve gradually rises until it reaches its peak at 18700 seconds (12:11 pm) for the reference panel, registering a temperature of 72.23°C. However, with cooling implemented at a flow rate of 0.35 L/M, the highest temperature achieved is 63.96°C. Similarly, at a flow rate of 0.7 L/M, the temperature decreases to 59.94°C, while at 1.4 L/M flow rate, it further reduces to 56.45°C. Consequently, the temperature curve exhibits a gradual descent owing to the decrease in the solar panel's temperature. The optimal cooling performance is observed when the flow rate is set at 1.4 L/M, and cooling efficiency diminishes as the flow rate is reduced. A comparative analysis with the reference plate confirms the effectiveness of the cooling system.

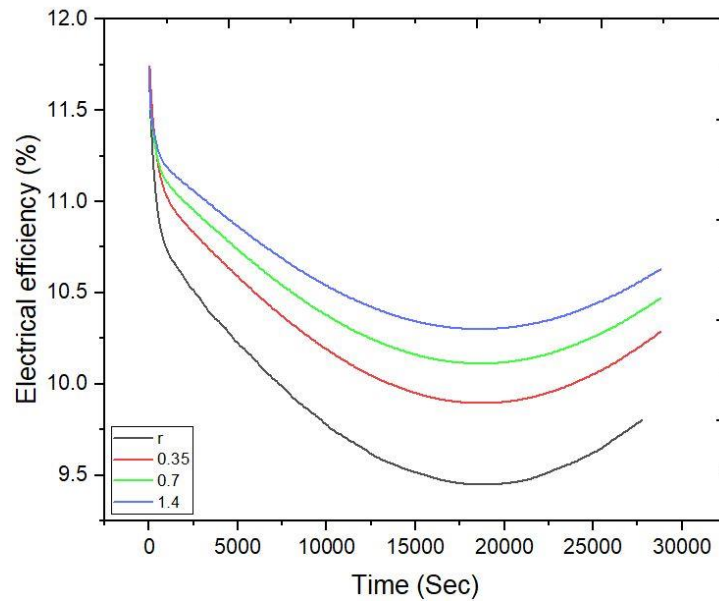


Figure 4.24. Variation in Electrical Efficiency with five-Channel Air Cooling.

Figure 4.24 demonstrates the gradual decrease in electrical efficiency, reaching its lowest point at 18700 seconds (12:11 pm) for the reference panel without any cooling, where the efficiency is recorded at 9.44%. In contrast, with cooling implemented at a flow rate of 0.35 L/M, the efficiency increases to 9.89%, while at a flow rate of 0.7 L/M, it further rises to 10.11%. The most significant enhancement in efficiency is achieved when the cooling is executed with a flow rate of 1.4 L/M, resulting in an efficiency of 10.30%. These results indicate that higher flow rates yield better cooling efficiency for the solar panel compared to the reference panel.

4.4.3. Seven Channel Model

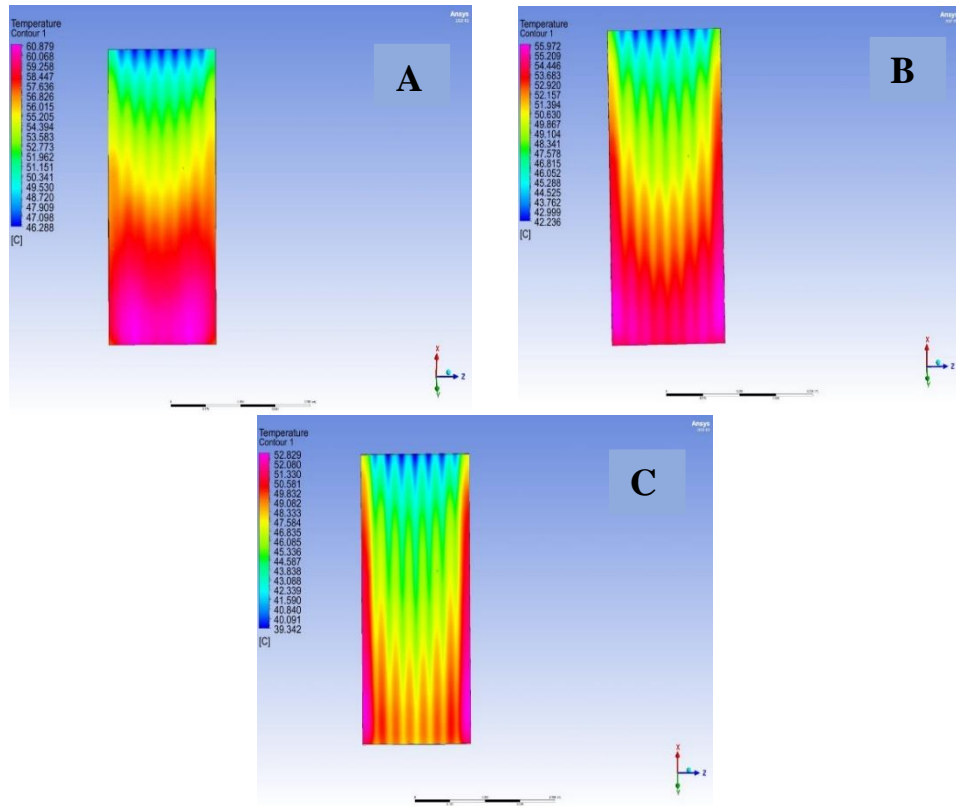


Figure 4.25. Temperature distribution on the solar panel utilizing a seven-channel cooling system a) for 0.35L/M, b) for 0.7L/M, c) for 1.4L/M.

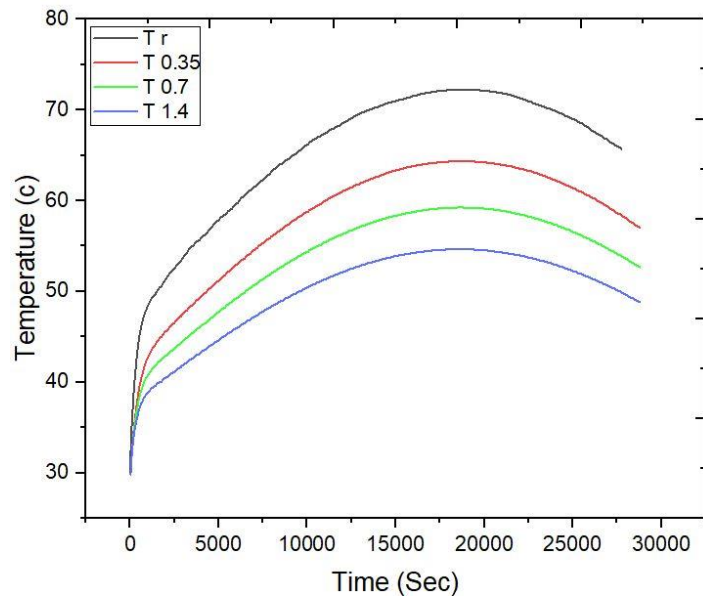


Figure 4.26. Variation in Temperature over time in the solar panel with seven-Channel Air Cooling.

Figure 4.26 illustrates the temporal variations in temperature of a solar panel under air cooling through a seven-channel configuration. The graph depicts the impact of cooling on maintaining the solar panel's temperature as compared to a scenario without any cooling. Initially, the temperature curve rises until it reaches its peak at 18700 seconds (12:11 pm), with the reference panel registering a temperature of 72.23°C. However, when subjected to cooling with a flow rate of 0.35 L/M, the temperature drops to 64.35°C. Further cooling with a flow rate of 0.7 L/M reduces the highest temperature to 59.25°C, and with a flow rate of 1.4 L/M, the highest temperature drops to 54.64°C. Subsequently, the temperature curve gradually descends due to the cooling effect on the solar panel. Notably, the most effective cooling is achieved when the flow rate is 1.4 L/M, and cooling efficiency decreases as the flow rate is reduced, relative to the reference panel.

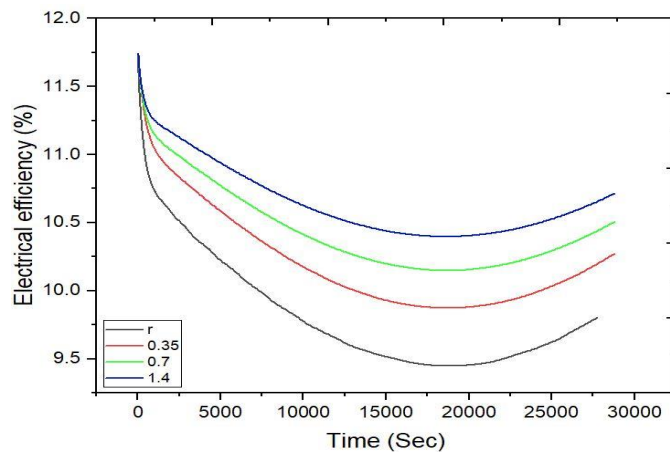


Figure 4.27. Variation in Electrical Efficiency with Seven-Channel Air Cooling.

Figure 4.27 presents the relationship between electrical efficiency and the solar panel's temperature under seven-channel air cooling conditions. The graph demonstrates the gradual decrease in electrical efficiency corresponding to the variation in the solar panel's temperature. The lowest efficiency is observed at 18700 seconds (12:11 pm) in the reference panel without cooling, measuring 9.44%. However, when cooling is applied with a flow rate of 0.35 L/M, the efficiency improves to 9.87%. Similarly, cooling with a flow rate of 0.7 L/M results in an efficiency of 10.15%, and with a flow rate of 1.4 L/M, the efficiency increases to 10.39%. Notably, higher flow rates lead to better cooling efficiency for the solar panel, outperforming the reference panel's efficiency.

4.4.4. Nine Channel Model

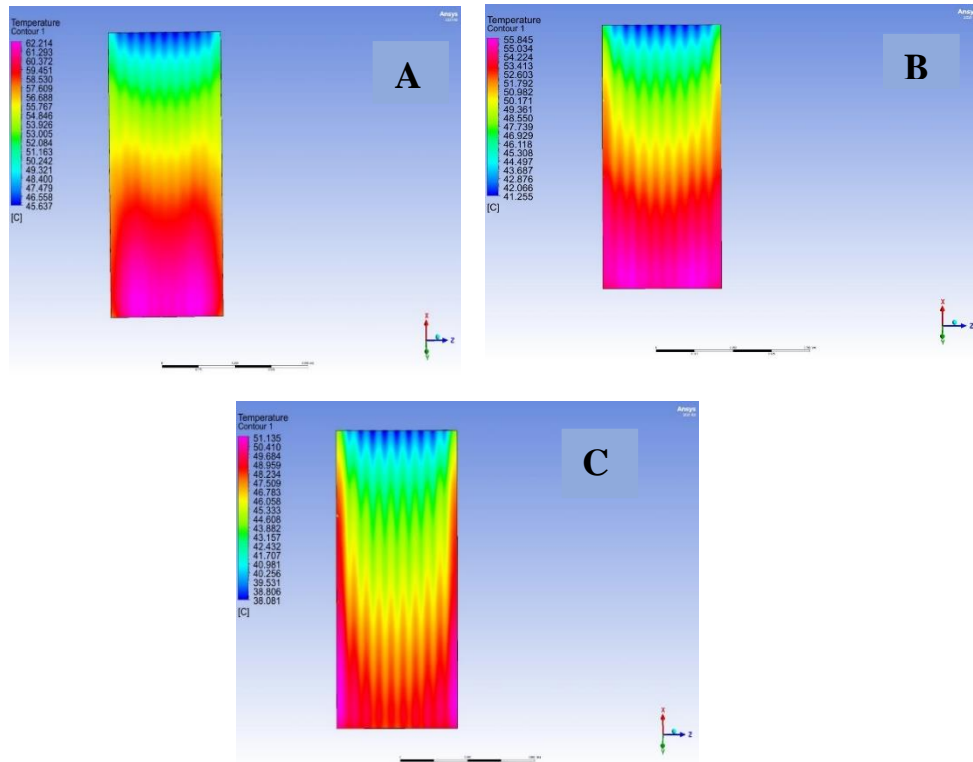


Figure 4.28. Temperature distribution on the solar panel utilizing a nine-channel cooling system a) for 0.35L/M, b) for 0.7L/M, c) for 1.4L/M.

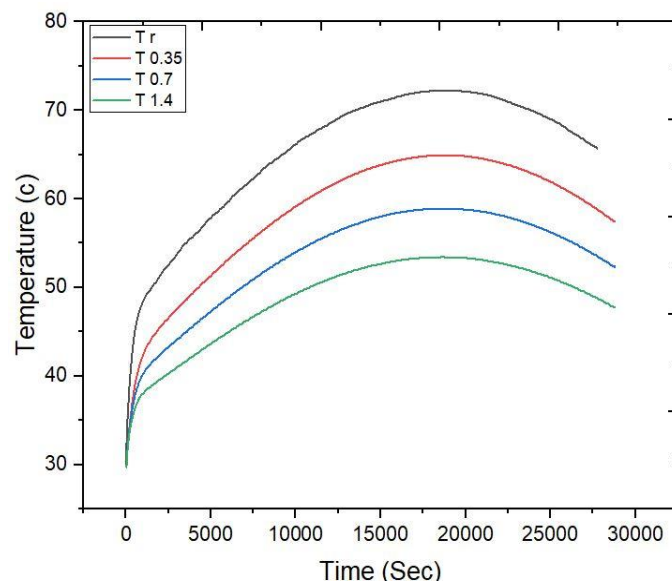


Figure 4.29. Variation in Temperature over time in the solar panel with nine-Channel Air Cooling.

Figure 4.29 illustrates the temporal variation in the temperature of a solar panel subjected to nine-channel air cooling. This figure demonstrates the impact of cooling on maintaining the solar panel's temperature in comparison to a scenario without cooling. The temperature curve exhibits an increasing trend until it reaches its peak at 18700 seconds (12:11 pm), with the reference temperature measured at 72.23°C. However, when cooling is applied with a flow rate of 0.35 L/M, the temperature lowers to 64.93°C. Further cooling with a flow rate of 0.7 L/M leads to a highest temperature of 58.91°C, while at a flow rate of 1.4 L/M, the highest temperature recorded is 53.43°C. Subsequently, the curve gradually descends as the solar panel's temperature decreases. The most effective cooling is achieved when the flow rate is 1.4 L/M, and cooling efficiency decreases as the flow rate is reduced. A comparison with the reference plate is performed.

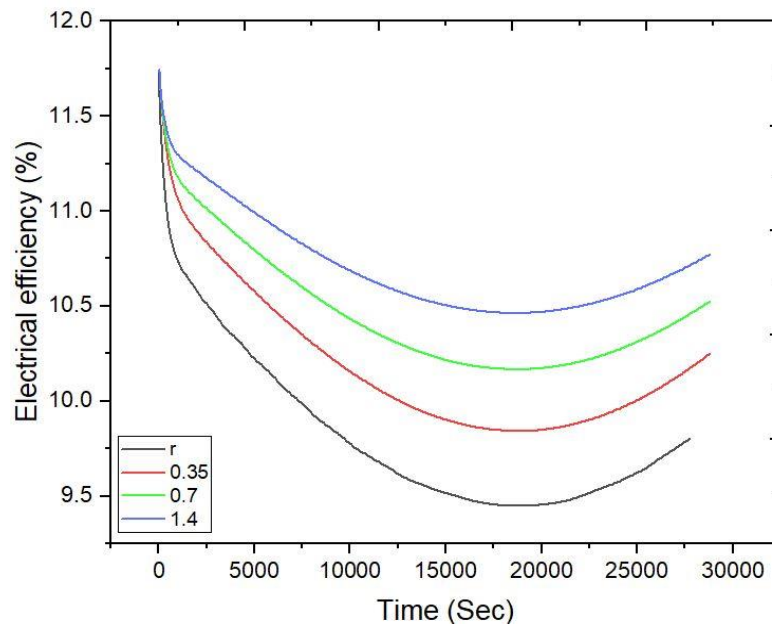


Figure 4.30. Variation in Electrical Efficiency with nine-Channel Air Cooling.

Figure 4.30 presents the variation in electrical efficiency resulting from the different temperatures of the solar panel with nine-channel air cooling. The electrical efficiency demonstrates a gradual decline, reaching its lowest value at 18700 seconds (12:11 pm) for the reference panel without cooling, registering at 9.44%. However, with cooling applied at a flow rate of 0.35 L/M, the efficiency increases to 9.84%, while at a flow rate of 0.7 L/M, it reaches 10.16%. The highest efficiency of 10.46% is achieved when

cooling is performed with a flow rate of 1.4 L/M. Notably, a higher flow rate corresponds to superior cooling efficiency of the solar panel compared to the reference panel.

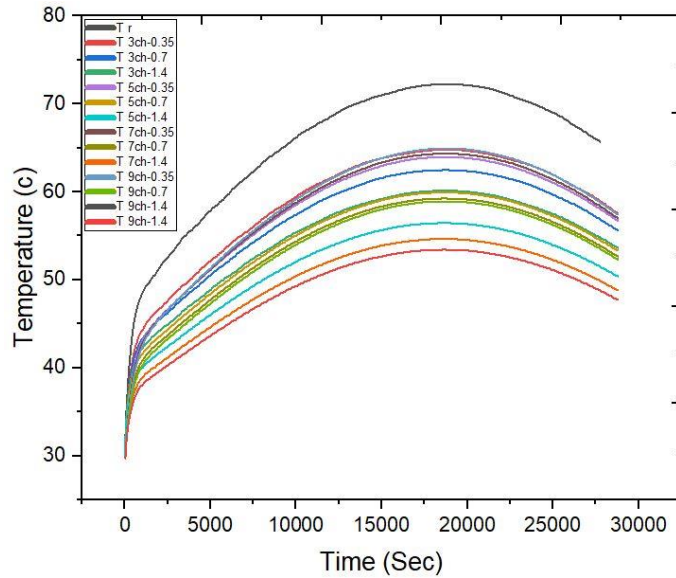


Figure 4.31. Variation in Temperature over time in the solar panel in the solar panel under different air-cooling configurations.

Figure 4.31 depicts the temporal temperature variations in the solar panel under different air-cooling configurations, namely the 9-channel, 7-channel, 5-channel, and 3-channel models, in comparison to the reference panel without any cooling.

The temperature differences observed among the various models highlight the cooling effectiveness in lowering the solar panel's temperature. Notably, the 9-channel model exhibits the most efficient cooling performance, followed by the 7-channel model, the 5-channel model, and lastly, the 3-channel model. This trend indicates that an increase in the number of channels correlates with improved cooling quality, thereby leading to reduced temperatures of the solar panel.

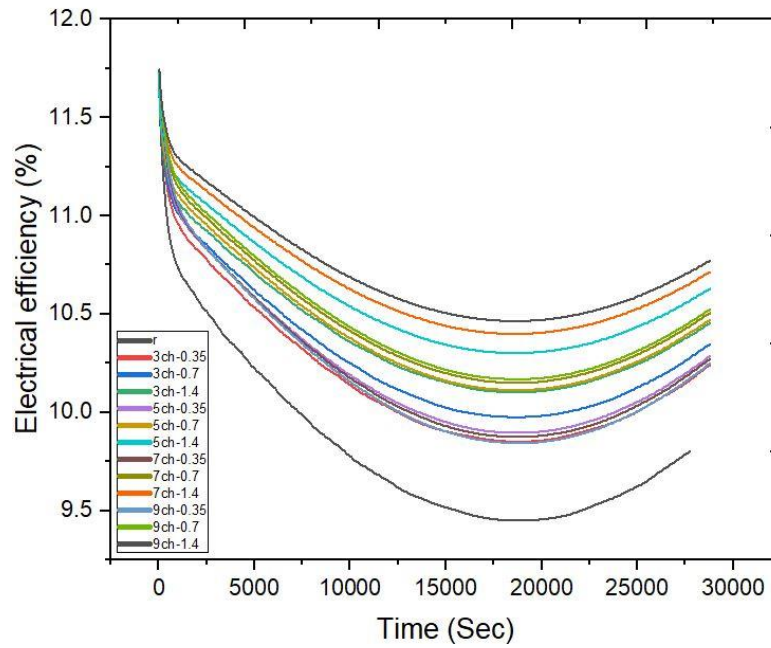


Figure 4.32. Variation in Electrical Efficiency in the solar panel under different air-cooling configurations

When comparing the reference panel without cooling to the solar panel with cooling, it is evident that the latter achieves higher electrical efficiency. Among the various air cooling configurations, the 9-channel model exhibits the highest electrical efficiency, followed by the 7-channel model, the 5-channel model, and finally the 3-channel model. This improvement in electrical efficiency is attributed to the temperature changes in the solar panel caused by the different cooling configurations.

4.5. OUTLET TEMPERATURE AVERAGE FOR COOLING CHANNELS

Table 4.1. Average Temperature for cooling channels

Type	Temperature (C)			
	3 channels	5 channels	7 channels	9 channels
Air Cooling				
0.35 L/M	46.2	52.984	55.969	58.073
0.7 L/M	38.578	44.717	47.242	48.947
1.4 L/M	34.29	37.483	39.293	40.465
Water Cooling				
0.35 L/M	41.27	40.081	39.913	39.851
0.7 L/M	39.682	39.712	39.751	39.789
1.4 L/M	39.25	39.416	39.59	39.658

4.6. COMPARISON BETWEEN WATER COOLING SYSTEM AND AIR COOLING SYST

This section presents a comparative analysis of the temperature and electrical efficiency changes in solar panels under water cooling and air-cooling systems. Figures 4.33 to 4.36 illustrate the temperature changes over time for solar panels subjected to different cooling methods, including three-channel, five-channel, seven-channel, and nine-channel air- and water-cooling systems.

Upon observation, it is evident that the reference panel, which experiences the direct impact of solar radiation, exhibits a gradual temperature increase until reaching its peak at 12:11 pm. The air-cooled panel displays lower temperatures compared to the reference panel due to its cooling effect. However, the difference becomes more pronounced when comparing the panels cooled by water. It is evident that water cooling yields superior results in terms of temperature reduction.

Additionally, Figures 4.37 to 4.40 depict the changes in electrical efficiency over time for the same configurations (three-channel, five-channel, seven-channel, and nine-channel) under both air- and water-cooling systems. These graphs demonstrate that cooling, regardless of the method, leads to an increase in electrical efficiency compared to the reference panel. While air cooling shows promising results, water cooling significantly outperforms air cooling in terms of enhancing electrical efficiency.

Furthermore, a comparative table (Table 4) is presented, juxtaposing the results of the current study using water as a coolant with those of another study [11] that employed water for cooling without refrigeration. The table presents flow rates, temperatures, and efficiency percentages for different cooling setups. The comparison shows that the current study achieved an efficiency rate of 9.82% with a corresponding temperature of 65.31°C in the nine-channel configuration using a flow rate of 1.4 L/M. In contrast, the other study recorded an efficiency rate of 14.36% with a temperature decrease of 23.55°C, utilizing cooling without refrigeration.

The disparity in results can be attributed to various factors, including the type of solar panel used, its geographical location, prevailing climate conditions, and specific cooling methods employed. In the present study, water cooling for the nine-channel configuration demonstrated a remarkable temperature reduction of 28.03°C, accompanied by a noteworthy increase in electrical efficiency by 1.42%. Conversely, the other study achieved a slightly lower efficiency increase of 1.53% alongside a temperature decrease of 23.55°C.

Overall, these findings emphasize the significance of carefully selecting appropriate cooling techniques based on the unique characteristics and requirements of the solar panel system in question.

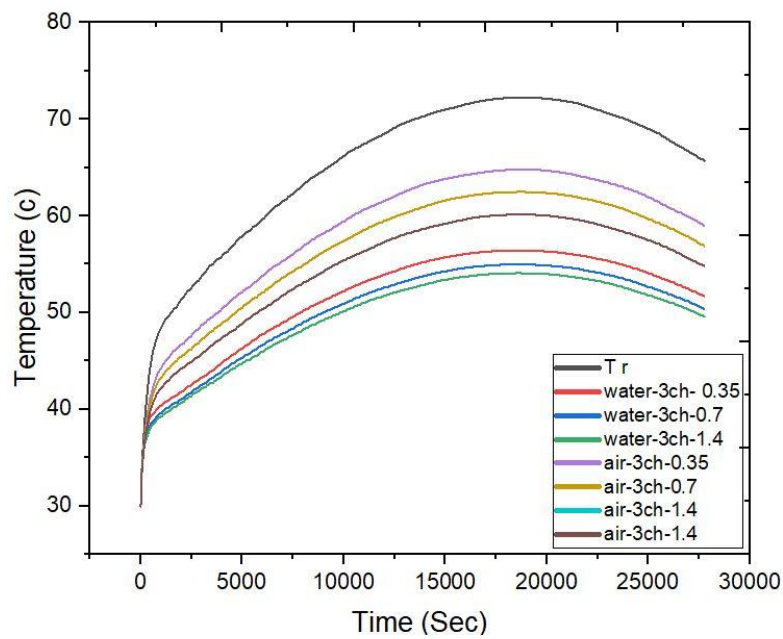


Figure 4.33. Time-dependent temperature variations in a solar panel with three-channel air and water cooling.

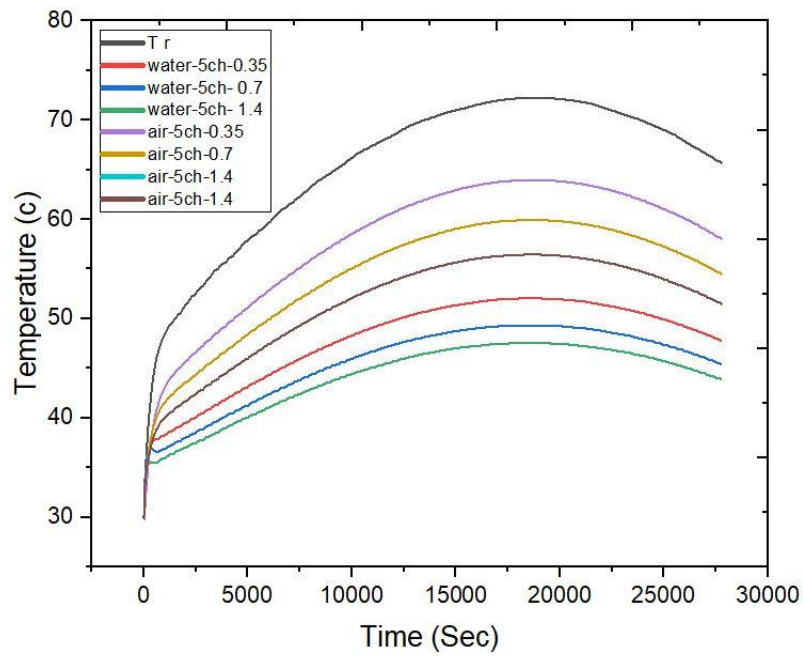


Figure 4.34. Time-dependent temperature variations in a solar panel with five-channel air and water cooling.

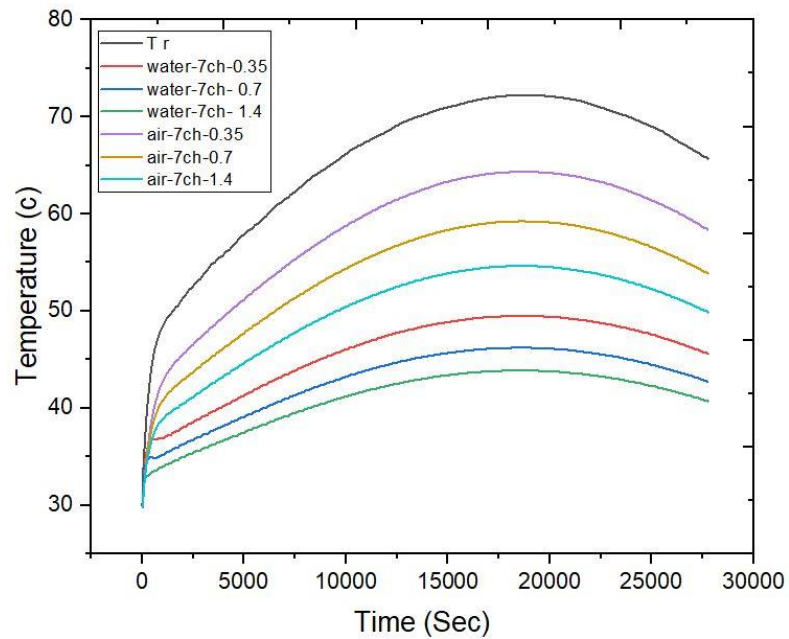


Figure 4.35. Time-dependent temperature variations in a solar panel with seven-channel air and water cooling.

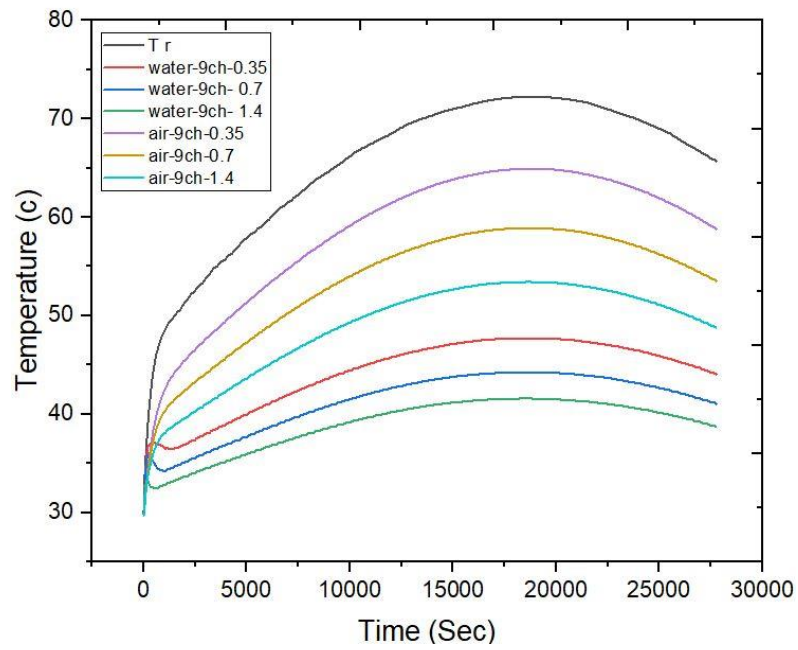


Figure 4.36. Time-dependent temperature variations in a solar panel with nine-channel air and water cooling.

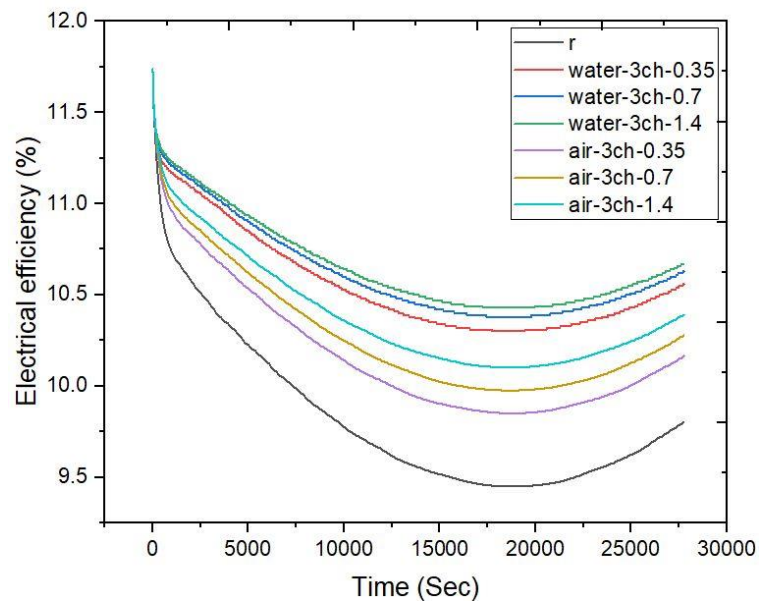


Figure 4.37. Electrical efficiency changes over time in a solar panel equipped with three-channel air and water cooling.

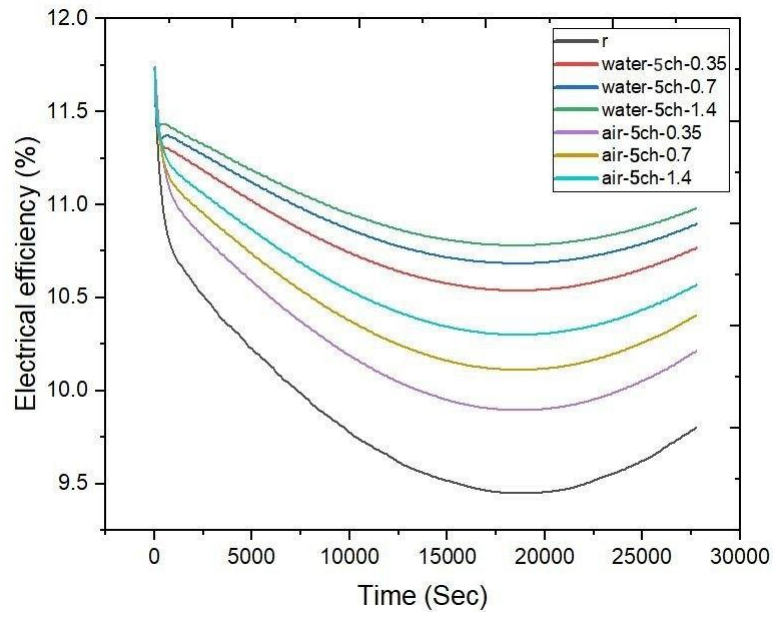


Figure 4.2. Electrical efficiency changes over time in a solar panel equipped with five-channel air and water cooling.

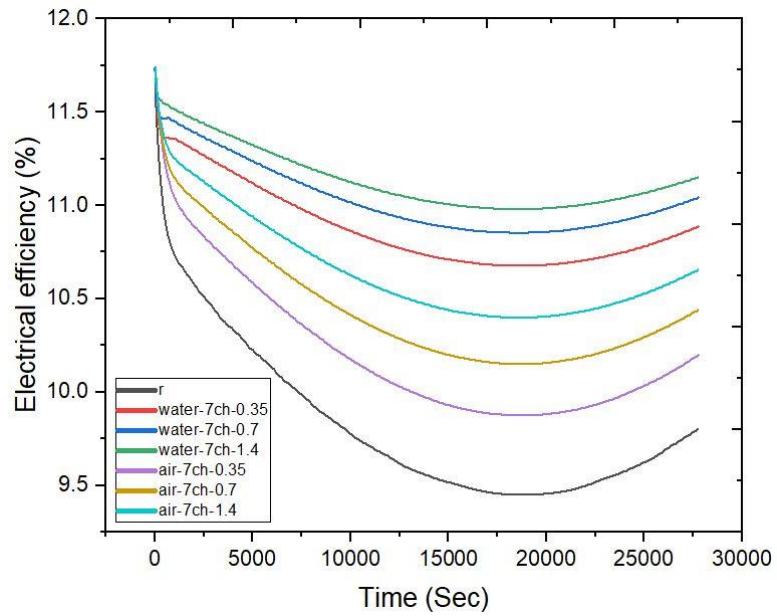


Figure 4.3. Electrical efficiency changes over time in a solar panel equipped with seven-channel air and water cooling.

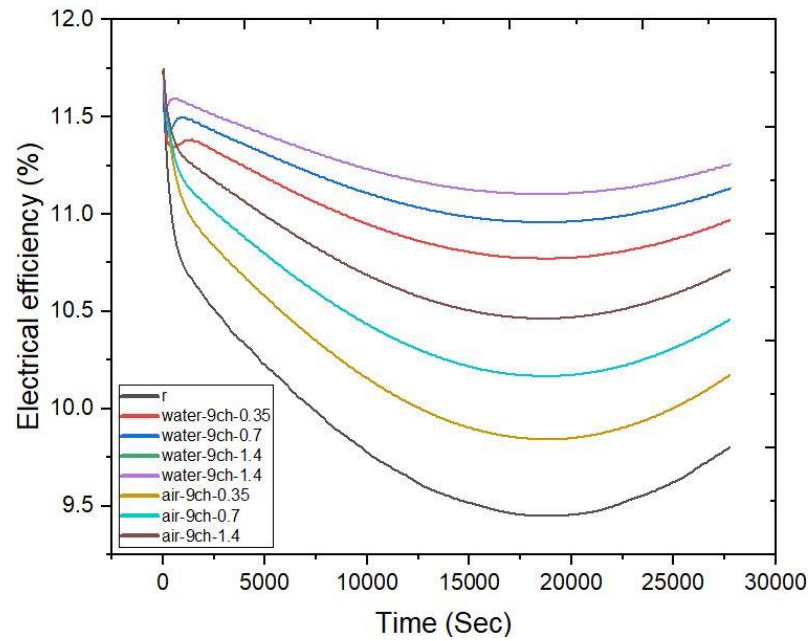


Figure 4.4. Electrical efficiency changes over time in a solar panel equipped with nine-channel air and water cooling.

Table 4.2. Comparison between this study and another study

My Study	Flow rate (L/M)	Temperature (C)				Efficiency %			
		3Ch	5Ch	7Ch	9Ch	3Ch	5Ch	7Ch	9Ch
	0.35	51.53	47.77	45.53	44.03	10.56	10.77	10.89	10.97
	0.7	50.31	45.51	42.78	41.13	10.6	10.89	11.03	11.12
	1.4	47.20	42.47	39.09	37.28	10.6	10.97	11.14	11.24
Another Study	-	With cooling		Without cooling		With cooling		Without cooling	
	-	35.72		59.27		14.36		12.83	

PART 5

CONCLUSION AND SUGGESTION

5.1. CONCLUSION

The results obtained from this study indicate that water cooling of solar panels yields superior outcomes in terms of both temperature regulation and electrical efficiency compared to air cooling. Moreover, it was observed that an increase in flow rate leads to a corresponding increase in the rate of temperature reduction. Notably, the flow rate of 1.4 L/m outperformed both 0.35 L/m and 0.7 L/m in terms of temperature reduction and electrical efficiency.

Furthermore, augmenting the number of channels proved to be beneficial for the models, with the most favorable results achieved when the number of channels was 9. Conversely, the least favorable outcomes were observed with only 3 channels utilized for cooling the solar panels.

Interestingly, specific time intervals were identified to record the highest temperatures and lowest electrical efficiency of the solar panel, notably at 12:11 pm.

Additionally, the relatively high temperature of the water retrieved from the cooling channels offers potential for alternative applications, such as utilizing it in solar heaters to enhance their thermal and electrical efficiency. Similarly, the hot air discharged from the channels can be employed for heating purposes.

5.2. SUGGESTION

Based on the findings of this study, several suggestions for further research and improvements can be made:

- Consider altering the number of channels and their dimensions in the models to explore their impact on cooling efficiency.
- Investigate the effects of changing the shape of the channels to vary the surface area in contact with the solar panel, thus potentially enhancing heat dissipation.
- Explore different fluid types and flow rates to optimize the cooling process.
- Conduct experiments with various metals for the channels to analyze their influence on heat transfer performance.
- Manipulate the distances between channels to assess their impact on cooling effectiveness.
- Investigate the influence of adjusting the angle of the solar panel on the cooling system's overall performance.

REFERENCES

1. Agyekum, E. B. and Velkin, V. I., "Optimization and techno-economic assessment of concentrated solar power (CSP) in South-Western Africa: A case study on Ghana", *Sustainable Energy Technologies And Assessments*, 40 (May): 100763 (2020).
2. Agyekum, E. B., Amjad, F., Mohsin, M., and Ansah, M. N. S., "A bird's eye view of Ghana's renewable energy sector environment: A Multi-Criteria Decision-Making approach", *Utilities Policy*, 70 (April): 101219 (2021).
3. Agyekum, E. B., Praveenkumar, S., Eliseev, A., and Velkin, V. I., "Design and construction of a novel simple and low-cost test bench point-absorber wave energy converter emulator system", *Inventions*, 6 (1): (2021).
4. Agyekum, E. B., Adebayo, T. S., Bekun, F. V., Kumar, N. M., and Panjwani, M. K., "Effect of two different heat transfer fluids on the performance of solar tower csp by comparing recompression supercritical co2 and rankine power cycles, china", *Energies*, 14 (12): (2021).
5. Adebayo, T. S., Agboola, M. O., Rjoub, H., Adeshola, I., Agyekum, E. B., and Kumar, N. M., "Linking economic growth, urbanization, and environmental degradation in China: What is the role of hydroelectricity consumption?", *International Journal Of Environmental Research And Public Health*, 18 (13): (2021).
6. Adebayo, T. S., Awosusi, A. A., Oladipupo, S. D., Agyekum, E. B., Jayakumar, A., and Kumar, N. M., "Dominance of fossil fuels in Japan's national energy mix and implications for environmental sustainability", *International Journal Of Environmental Research And Public Health*, 18 (14): (2021).
7. Homadi, A., Hall, T., and Whitman, L., "Study a novel hybrid system for cooling solar panels and generate power", *Applied Thermal Engineering*, 179 (May): 115503 (2020).
8. Alwan, N. T., Shcheklein, S. E., and Ali, O. M., "Experimental investigation of modified solar still integrated with solar collector", *Case Studies In Thermal Engineering*, 19 (February): 100614 (2020).
9. Alwan, N. T., Shcheklein, S. E., and Ali, O. M., "Experimental analysis of thermal performance for flat plate solar water collector in the climate conditions of Yekaterinburg, Russia", *Materials Today: Proceedings*, 42: 2076–2083 (2021).
10. Skoplaki, E. and Palyvos, J. A., "On the temperature dependence of photovoltaic module electrical performance: A review of efficiency/power correlations", *Solar*

Energy, 83 (5): 614–624 (2009).

11. Agyekum, E. B., PraveenKumar, S., Alwan, N. T., Velkin, V. I., and Shcheklein, S. E., "Effect of dual surface cooling of solar photovoltaic panel on the efficiency of the module: experimental investigation", *Heliyon*, 7 (9): e07920 (2021).
12. Dimri, N., Tiwari, A., and Tiwari, G. N., "Comparative study of photovoltaic thermal (PVT) integrated thermoelectric cooler (TEC) fluid collectors", *Renewable Energy*, 134: 343–356 (2019).
13. Shyam, Tiwari, G. N., and Al-Helal, I. M., "Analytical expression of temperature dependent electrical efficiency of N-PVT water collectors connected in series", *Solar Energy*, 114: 61–76 (2015).
14. Abdolzadeh, M. and Ameri, M., "Improving the effectiveness of a photovoltaic water pumping system by spraying water over the front of photovoltaic cells", *Renewable Energy*, 34 (1): 91–96 (2009).
15. Moharram, K. A., Abd-Elhady, M. S., Kandil, H. A., and El-Sherif, H., "Nels by water cEnhancing the performance of photovoltaic paooling", *Ain Shams Engineering Journal*, 4 (4): 869–877 (2013).
16. Yesildal, F., Ozakin, A. N., and Yakut, K., "Optimization of operational parameters for a photovoltaic panel cooled by spray cooling", *Engineering Science And Technology, An International Journal*, 25: 100983 (2022).
17. Siecker, J., Kusakana, K., and Numbi, B. P., "A review of solar photovoltaic systems cooling technologies", *Renewable And Sustainable Energy Reviews*, 79 (July 2016): 192–203 (2017).
18. Laseinde, O. T. and Ramere, M. D., "Efficiency Improvement in polycrystalline solar panel using thermal control water spraying cooling", *Procedia Computer Science*, 180: 239–248 (2021).
19. Xu, Y., Li, J., Tan, Q., Peters, A. L., and Yang, C., "Global status of recycling waste solar panels: A review", *Waste Management*, 75: 450–458 (2018).
20. Wang, Y., Zhou, S., and Huo, H., "Cost and CO2 reductions of solar photovoltaic power generation in China: Perspectives for 2020", *Renewable And Sustainable Energy Reviews*, 39 (2014): 370–380 (2014).
21. Karthick, S. N., Hemalatha, K. V., Balasingam, S. K., Manik Clinton, F., Akshaya, S., and Kim, H. J., "Dye-sensitized solar cells: History, components, configuration, and working principle", *Interfacial Engineering In Functional Materials For Dye-Sensitized Solar Cells*, 1–16 (2019).
22. Ingegneria, F., Magistrale, L., Di, M., In, S., Resistive, M., and Della, R., "Politecnico di milano", 1–11 (2012).
23. Özkul, F. B., Kayabasi, E., Çelik, E., Kurt, H., and Arcaklioğlu, E., "Investigating the effects of cooling options on photovoltaic panel efficiency: State of the art and

future plan", *PVCon 2018 - International Conference On Photovoltaic Science And Technologies*, 1–6 (2018).

24. Li, D., King, M., Dooner, M., Guo, S., and Wang, J., "Study on the cleaning and cooling of solar photovoltaic panels using compressed airflow", *Solar Energy*, 221 (March): 433–444 (2021).
25. Al-Amri, F., Maatallah, T. S., Al-Amri, O. F., Ali, S., Ali, S., Ateeq, I. S., Zachariah, R., and Kayed, T. S., "Innovative technique for achieving uniform temperatures across solar panels using heat pipes and liquid immersion cooling in the harsh climate in the Kingdom of Saudi Arabia", *Alexandria Engineering Journal*, 61 (2): 1413–1424 (2022).
26. Almuwailhi, A. and Zeitoun, O., "Investigating the cooling of solar photovoltaic modules under the conditions of Riyadh", *Journal Of King Saud University - Engineering Sciences*, (xxxx): (2021).
27. Soliman, A. M. A., Hassan, H., and Ookawara, S., "An experimental study of the performance of the solar cell with heat sink cooling system", *Energy Procedia*, 162: 127–135 (2019).
28. Ramesh, C., Vijayakumar, M., Alshahrani, S., Navaneethakrishnan, G., Palanisamy, R., Natrayan, L., Saleel, C. A., Afzal, A., Shaik, S., and Panchal, H., "Performance enhancement of selective layer coated on solar absorber panel with reflector for water heater by response surface method: A case study", *Case Studies In Thermal Engineering*, 36 (February): 102093 (2022).
29. Ayed, H., Moria, H., Aldawi, F., Farouk, N., Sharma, K., Youshanlouei, M. M., Mahariq, I., and Jarad, F., "Thermal, efficiency and power output evaluation of pyramid, hexagonal and conical forms as solar panel", *Case Studies In Thermal Engineering*, 27 (March): 101232 (2021).
30. Drame, M. S., Diop, D., Talla, K., Diallo, M., Ngom, B. D., and Nebon, B., "Structural and physicochemical properties of dust collected on PV panels surfaces and their potential influence on these solar modules efficiency in Dakar, Senegal, West Africa", *Scientific African*, 12: e00810 (2021).
31. Sodhi, M., Banaszek, L., Magee, C., and Rivero-Hudec, M., "Economic Lifetimes of Solar Panels", *Procedia CIRP*, 105: 782–787 (2022).
32. Tian, M. W., Khetib, Y., Yan, S. R., Rawa, M., Sharifpur, M., Cheraghian, G., and Melaibari, A. A., "Energy, exergy and economics study of a solar/thermal panel cooled by nanofluid", *Case Studies In Thermal Engineering*, 28: 101481 (2021).
33. Setiyo, M., Waluyo, B., Widodo, N., Rochman, M. L., Munahar, S., and Fatmaryanti, S. D., "Cooling effect and heat index (HI) assessment on car cabin cooler powered by solar panel in parked car", *Case Studies In Thermal Engineering*, 28 (June): 101386 (2021).
34. Madurai Elavarasan, R., Mudgal, V., Selvamanohar, L., Wang, K., Huang, G.,

- Shafiullah, G. M., Markides, C. N., Reddy, K. S., and Nadarajah, M., "Pathways toward high-efficiency solar photovoltaic thermal management for electrical, thermal and combined generation applications: A critical review", *Energy Conversion And Management*, 255 (February): 115278 (2022).
35. Salehi, R., Jahanbakhshi, A., Reza Golzarian, M., and Khojastehpour, M., "Evaluation of solar panel cooling systems using anodized heat sink equipped with thermoelectric module through the parameters of temperature, power and efficiency", *Energy Conversion And Management: X*, 11 (April): 100102 (2021).
 36. Zubeer, S. A. and Ali, O. M., "Experimental and numerical study of low concentration and water-cooling effect on PV module performance", *Case Studies In Thermal Engineering*, 34 (April): 102007 (2022).
 37. Moh, T. S. Y., Ting, T. W., and Lau, A. H. Y., "Graphene Nanoparticles (GNP) nanofluids as key cooling media on a flat solar panel through micro-sized channels", *Energy Reports*, 6: 282–286 (2020).
 38. Murtadha, T. K., dil Hussein, A. A., Alalwany, A. A. H., Alrwashdeh, S. S., and Al-Falahat, A. M., "Improving the cooling performance of photovoltaic panels by using two passes circulation of titanium dioxide nanofluid", *Case Studies In Thermal Engineering*, 36 (May): 102191 (2022).
 39. Zhao, X., Aili, A., Zhao, D., Xu, D., Yin, X., and Yang, R., "Dynamic glazing with switchable solar reflectance for radiative cooling and solar heating", *Cell Reports Physical Science*, 3 (4): 100853 (2022).
 40. Haidar, Z. A., Orfi, J., and Kaneesamkandi, Z., "Experimental investigation of evaporative cooling for enhancing photovoltaic panels efficiency", *Results In Physics*, 11 (May): 690–697 (2018).
 41. Mohan, V., D.S., H. R., Patil, G., M., J., Unni, R. C., K., N., Thirumala, K., and Bu, S., "Policy assistance for adoption of residential solar PV in India: A stakeholder-centric approach for welfare optimization", *Energy Reports*, 8: 197–206 (2022).
 42. Jelonek, Z., Drobniak, A., Mastalerz, M., and Jelonek, I., "Jo ur na l P re of", *Science Of The Total Environment*, 141267 (2020).
 43. Gomaa, M. R., Ahmed, M., and Rezk, H., "Temperature distribution modeling of PV and cooling water PV/T collectors through thin and thick cooling cross-fined channel box", *Energy Reports*, 8: 1144–1153 (2022).
 44. Tahir, F., Baloch, A. A. B., and Al-Ghamdi, S. G., "Impact of climate change on solar monofacial and bifacial Photovoltaics (PV) potential in Qatar", *Energy Reports*, 8: 518–522 (2022).
 45. Kara, K., Abby, C., and Jadon, J., "Feasibility of Combining Solar Panels and Green Roofs on the Activities and Recreation Center", 1–22 (2017).
 46. Zhang, Y., Wang, W., Wang, Z., Gao, M., Zhu, L., and Song, J., "Green building

design based on solar energy utilization: Take a kindergarten competition design as an example", *Energy Reports*, 7: 1297–1307 (2021).

47. Ko, B., Lee, D., Badloe, T., and Rho, J., "Metamaterial-based radiative cooling: Towards energy-free all-day cooling", *Energies*, 12 (1): 1–14 (2019).
48. Yu, J., Tang, Y. M., Chau, K. Y., Nazar, R., Ali, S., and Iqbal, W., "Role of solar-based renewable energy in mitigating CO2 emissions: Evidence from quantile-on-quantile estimation", *Renewable Energy*, 182: 216–226 (2022).
49. Güney, T., "Solar energy, governance and CO2 emissions", *Renewable Energy*, 184: 791–798 (2022).
50. Zamrodah, Y., "濟無No Title No Title No Title", 1–23 (2016).
51. "Chapter 3 Continuous Random Variables 3.1 Introduction", .
52. Shen, C., Zhang, Y., Zhang, C., Pu, J., Wei, S., and Dong, Y., "A numerical investigation on optimization of PV/T systems with the field synergy theory", *Applied Thermal Engineering*, 185 (October 2020): 116381 (2021).

RESUME

Mujtaba Jalal Khazaal AL-MOHAMMEDAWI, graduated from primary and secondary schools in this city. I started studying at the University of Technology in Baghdad in 2014-2015, graduated from the university in 2018-2019, and started working in Karbuk in 2022.